Myoplasmic Calcium Transients in Intact Frog Skeletal Muscle Fibers Monitored with the Fluorescent Indicator Furaptra

M. KONISHI, S. HOLLINGWORTH, A. B. HARKINS, and S. M. BAYLOR

From the Department of Physiology, University of Pennsylvania Medical Center, Philadelphia, Pennsylvania 19104-6085; and Department of Physiological Sciences, The Medical School, Framlington Place, University of Newcastle, Newcastle upon Tyne, United Kingdom

ABSTRACT Furaptra (Raju, B., E. Murphy, L. A. Levy, R. D. Hall, and R. E. London. 1989. *Am. J. Physiol.* 256:C540–C548) is a "tri-carboxylate" fluorescent indicator with a chromophore group similar to that of fura-2 (Grynkiewicz, G., M. Poenie, and R. Y. Tsien. 1985. *J. Biol. Chem.* 260:3440–3450). In vitro calibrations indicate that furaptra reacts with Ca^{2+} and Mg^{2+} with 1:1 stoichiometry, with dissociation constants of 44 μM and 5.3 mM, respectively (16–17°C; ionic strength, 0.15 M; pH, 7.0). Thus, in a frog skeletal muscle fiber stimulated electrically, the indicator is expected to respond to the change in myoplasmic free $[Ca^{2+}]$ ($\Delta[Ca^{2+}]$) with little interference from changes in myoplasmic free $[Mg^{2+}]$. The apparent longitudinal diffusion constant of furaptra in myoplasm was found to be 0.68 (±0.02, SEM) × 10^{-6} cm^2 s^{-1} (16–16.5°C), a value which suggests that about half of the indicator was bound to myoplasmic constituents of large molecular weight. Muscle membranes (surface and/or transverse-tubular) appear to have some permeability to furaptra, as the total quantity of indicator contained within a fiber decreased after injection; the average time constant of the loss was 302 (±145, SEM) min. In fibers containing <0.5 mM furaptra and stimulated by a single action potential, the calibrated peak value of $\Delta[Ca^{2+}]$ averaged 5.1 (±0.3, SEM) μM. This value is about half that reported in the preceding paper (9.4 μM; Konishi, M., and S. M. Baylor. 1991. *J. Gen. Physiol.* 97:245–270) for fibers injected with purpurate-diacetic acid (PDAA). The latter difference may be explained, at least in part, by the likelihood that the effective dissociation constant of furaptra for Ca^{2+} is larger in vivo than in vitro, owing to the binding of the indicator to myoplasmic constituents. The time course of furaptra's $\Delta[Ca^{2+}]$, with average values (±SEM) for time to peak and half-width of 6.3 (±0.1) and 9.5 (±0.4) ms, respectively, is very similar to that of $\Delta[Ca^{2+}]$ recorded with PDAA. Since furaptra's $\Delta[Ca^{2+}]$ can be recorded at a single excitation wavelength (e.g., 420 nm) with little interference from fiber intrinsic

Address reprint requests to Dr. S. M. Baylor, Department of Physiology, University of Pennsylvania Medical Center, Philadelphia, PA 19104-6085.

Dr. Konishi's current address is Department of Physiology, The Jikei University School of Medicine, 3-25-8 Nishishinbashi, Minato-Ku, Tokyo 105, Japan.

J. GEN. PHYSIOL. © The Rockefeller University Press · 0022-1295/91/02/0271/31 $2.00
Volume 97 February 1991 271–301

changes, movement artifacts, or $\Delta[Mg^{2+}]$, furaptra represents a useful myoplasmic Ca^{2+} indicator, with properties complementary to those of other available indicators.

INTRODUCTION

The preceding article (Konishi and Baylor, 1991) described some of the advantages and disadvantages of using purpurate diacetic acid (PDAA; Hirota et al., 1989) to monitor the myoplasmic free Ca^{2+} transient ($\Delta[Ca^{2+}]$) in intact frog skeletal muscle fibers. This article describes the use of the fluorescent compound furaptra (Raju et al., 1989) for a similar purpose.

Furaptra is optically similar to fura-2 (Grynkiewicz et al., 1985), but has a dissociation constant (K_d) for Ca^{2+} in the range of 40–50 μM, i.e., ~250 times higher than that of fura-2 and ~20-fold lower than that of PDAA. Thus, furaptra's K_d is well suited for detecting a $\Delta[Ca^{2+}]$ in peak value of 9–10 μM, the average value measured in intact frog twitch fibers with PDAA (Konishi and Baylor, 1991). Furaptra has the potential disadvantage of not being completely selective for Ca^{2+} over Mg^{2+}, with a reported K_d for Mg^{2+} in the low millimolar range (Raju et al., 1989); i.e., several times less than that of fura-2. (With PDAA, K_d for Mg^{2+} is very large and has not been accurately measured). Thus, based on dissociation constants measured in vitro, furaptra is expected to be a useful indicator of myoplasmic free $[Mg^{2+}]$ in resting muscle fibers and of $\Delta[Ca^{2+}]$ in fibers stimulated electrically.

This article focuses on the $\Delta[Ca^{2+}]$ signal from furaptra detected in response to action potential stimulation and compares this indicator's signal with that of PDAA, antipyrylazo III, fura-2, and azo-1. The results show that the fluorescence change from furaptra monitors $\Delta[Ca^{2+}]$ with properties complementary to those available from the other indicators. For example, because it reports $\Delta[Ca^{2+}]$ as a change in fluorescence (as does fura-2), furaptra's signal can be recorded without interference from fiber intrinsic changes and with relatively little interference from movement artifacts. However, in contrast to fura-2, the kinetics of furaptra's reaction with Ca^{2+} under intracellular conditions appear to be of sufficient speed that $\Delta[Ca^{2+}]$ is monitored with little or no kinetic delay. Because of these features, furaptra will probably prove to be an indicator with considerable utility in future studies of $\Delta[Ca^{2+}]$ in skeletal muscle and possibly other preparations.

A preliminary account of some of the results has appeared in abstract form (Baylor et al., 1989; Konishi et al., 1989, 1990).

METHODS

In Vitro Calibrations with Furaptra

Furaptra was obtained from Molecular Probes, Inc. (Eugene, OR) as the tetra-potassium salt of "Mag-fura-2." Previous in vitro calibrations (Raju et al., 1989) were based on fluorescence measurements carried out at 37°C. We have carried out analogous calibrations, based primarily on absorbance measurements, at 16–17°C, the temperature of our in vivo experiments. Our standard buffer solution contained (in mM): 120 KCl, 10 NaCl, and 10 PIPES (potassium salt of piperazine-*N*,*N*′-bis[2-ethane-sulfonic acid]), pH 7.0. For the titrations with Mg^{2+}, freshly purchased crystals of $MgCl_2{:}6H_2O$ (Sigma Chemical Co., St. Louis, MO) were used. For these titrations, the buffer solution also contained 0.2 mM EGTA to complex contaminant Ca^{2+} (present at 1–10 μM as separately estimated with fura-2 for each buffer solution), and possibly

other divalent ions. Since the K_d of EGTA for Mg^{2+} is large, ~49 mM at 16.5°C (Martell and Smith, 1974), the quantity of Mg^{2+} complexed by EGTA was small (<0.5% of added Mg^{2+}). For the titrations with Ca^{2+}, a certified 1 M stock solution of $CaCl_2$ was used (BDH Chemicals Ltd., Poole, UK). In cases where the free concentration of Ca^{2+} ($[Ca^{2+}]$) was set with 10 mM HEDTA buffer (*N*-hydroxy-ethylethylene diamine-triacetic acid), the concentration of KCl was reduced to 90 mM. For calculation of $[Ca^{2+}]$, an apparent K_d of 5.62 μM was assumed for the Ca^{2+}-HEDTA reaction at 0.15 M ionic strength and 16.5°C (Martell and Smith, 1974). In all

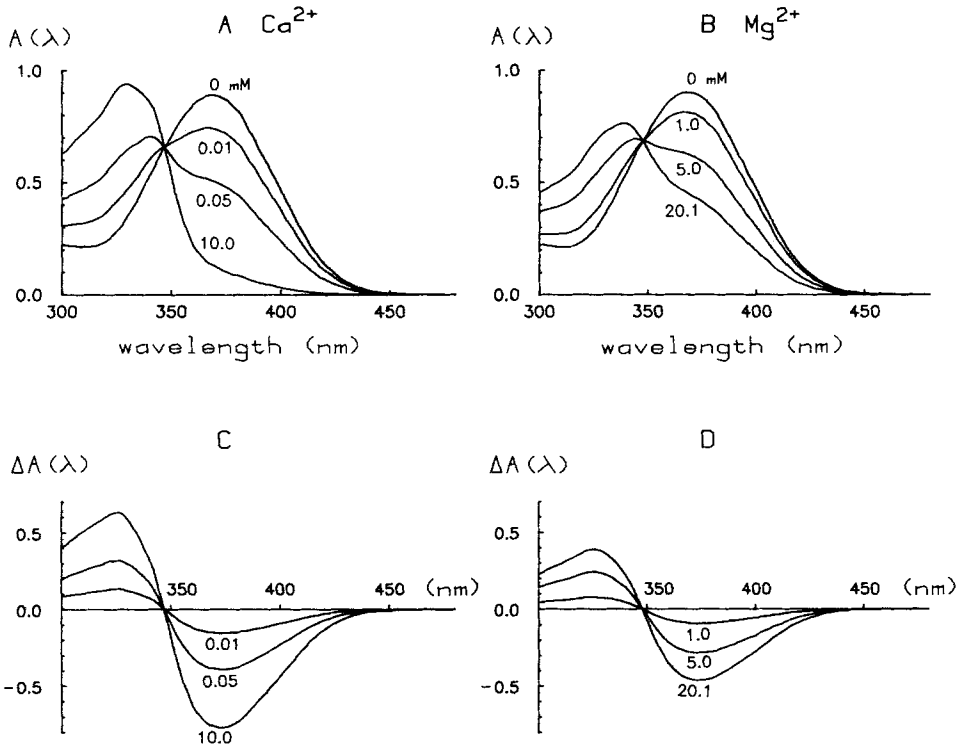

FIGURE 1. In vitro absorbance spectra of 30 μM furaptra in a 1-cm quartz cuvette (16–17°C). Titrations with Ca^{2+} are shown in *A* and *C*, and with Mg^{2+} in *B* and *D*. The upper panels show absolute spectra, with the free divalent ion concentrations indicated in millimolar next to the curves. The lower panels show difference spectra, i.e., the changes relative to the metal-free spectrum. The spectra were measured on a scanning spectrophotometer (model 4050; LKB Instruments, Inc., Gaithersburg, MD) and digitally processed as described in Hollingworth et al. (1987).

cases, $[Ca^{2+}]$ and $[Mg^{2+}]$ (the free concentration of Mg^{2+}) were calculated from the total added concentration of divalent ions minus the concentrations calculated to be bound, either to furaptra itself or to the added chelators HEDTA or EGTA.

The upper panels of Fig. 1 show examples of absorbance spectra of furaptra measured in the presence of various concentrations of $[Ca^{2+}]$ (*A*) or $[Mg^{2+}]$ (*B*), indicated in millimolar next to the curves. The shapes of the curves, particularly those for Ca^{2+}, are generally similar to fura-2's absorbance spectra (see, for example, Baylor and Hollingworth, 1988).

The first goal of our in vitro measurements was to determine the extinction coefficients of furaptra so that both in vitro and in vivo concentrations of the dye could be estimated by Beer's law. The experimental method used, which assumes 1:1 stoichiometry for the Ca^{2+}-furaptra reaction (cf. below), was the same as given by Baylor and Hollingworth (1988) for estimation of the extinction coefficients for fura-2. For furaptra, the method indicated that at 420 nm, $\epsilon_D(420)$, the extinction coefficient of metal-free furaptra, and $\Delta\epsilon_{CaD}(420)$, the change in extinction coefficient of furaptra upon complexation with Ca^{2+}, are, respectively, 4.65×10^3 M^{-1} cm^{-1} and -4.47×10^3 M^{-1} cm^{-1}. From the value of $\epsilon_D(420)$ and the shape of the metal-free spectra shown in Fig. 1, $\epsilon_D(368)$, the extinction coefficient of metal-free furaptra at 368 nm (the wavelength where the absorbance of metal-free furaptra is maximum) is estimated to be 3.01×10^4 M^{-1} cm^{-1}.

The lower parts of Fig. 1 show the difference spectra for Ca^{2+} (*C*) and Mg^{2+} (*D*), obtained by

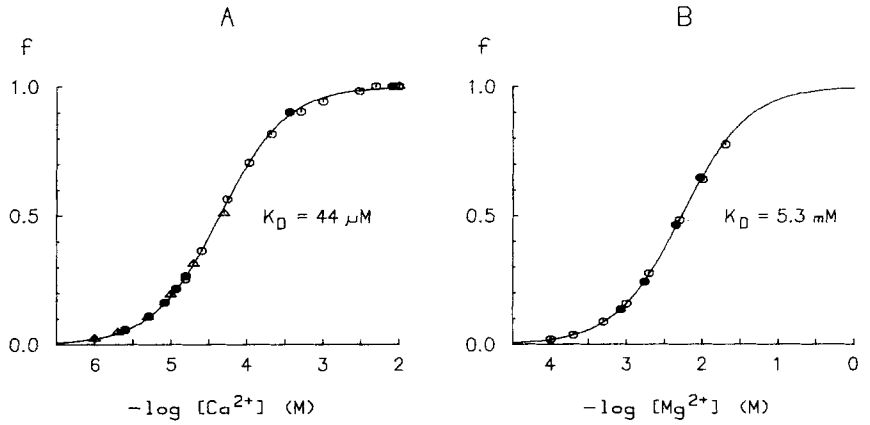

FIGURE 2. Analysis of the in vitro changes seen in Fig. 1 and other titrations (not shown) in terms of a 1:1 binding reaction of furaptra with Ca^{2+} (*A*) or Mg^{2+} (*B*). The ordinate estimates the fraction of the indicator in the metal-bound form as a function of the free metal concentration expressed on a $\log_{10}$ scale (abscissa). The fitted values of K_d are shown on the graphs. Open symbols were obtained in titrations at low indicator concentration (0.03 mM) in a 1-cm cuvette, whereas filled symbols were obtained at high indicator concentration (*A*, 1.84 mM; *B*, 1.07 mM) in a 1-mm cuvette. HEDTA (see Methods) was used to set free [Ca^{2+}] for the open triangle measurements in *A*.

subtraction of the metal-free spectra from the other spectra in the upper parts. Within either *C* or *D*, the curves have an identical shape; i.e., they differ only by a scaling constant, as expected if furaptra forms a single stoichiometric complex with either ion (Ca^{2+} or Mg^{2+}). A precise comparison of the curves in *C* with those in *D* (and other measurements not shown) indicates that there is a small but consistent difference in the shape of the Ca^{2+} and Mg^{2+} difference spectra; for example, the isosbestic wavelength of the Ca^{2+} difference spectrum is 347 nm, whereas that for Mg^{2+} is 348 nm. Nevertheless, the close similarity of the basic shapes of the difference spectra for the two ions suggests that Ca^{2+} and Mg^{2+} interact with furaptra at the same binding site and with the same stoichiometry.

In Fig. 2 the relative amplitudes (symbols) of these and other difference spectra have been least-squares fitted under the assumption of 1:1 stoichiometry (Raju et al., 1989), in *A* for the titrations with Ca^{2+} and in *B* for those with Mg^{2+}. The curve-fitting procedure was identical to

that described in connection with Eq. 1 of the preceding paper (Konishi and Baylor, 1991) and involved least-squares adjustment of two parameters: the maximal amplitude of the difference spectrum (i.e., extrapolated to saturating [Ca^{2+}] or [Mg^{2+}]) and the 1:1 dissociation constant (K_d) for the reaction. The fitted values of K_d were 44 μM for Ca^{2+} (*A*) and 5.3 mM for Mg^{2+} (*B*). With each ion, a single value of K_d was found to fit the titration data at both low and high furaptra concentrations (0.03 and 1.1–1.8 mM; see legend of Fig. 2), thus confirming that the stoichiometric complex formed is probably 1:1.

The values of ϵ_D and $\Delta\epsilon_{CaD}$ given above indicate that at 420 nm the absorbance of furaptra in the Ca^{2+}-bound form is only 4% of that in the metal-free form. From Figs. 1 *B* and 2 *B*, $\Delta\epsilon_{MgD}$ (the change in extinction coefficient of furaptra with Mg^{2+}-complexation) is estimated to be -3.62×10^3 M^{-1} cm^{-1} at 420 nm. This, in turn, implies that the absorbance of furaptra in the Mg^{2+}-bound form is 22% of the absorbance of metal-free furaptra (i.e., $\epsilon_{MgD}(420)/\epsilon_D(420) = 0.22$).

A comparison of our absorbance calibrations at 16.5°C with the fluorescence calibrations of Raju et al. (1989) at 37°C (but at similar solution pH and ionic strength) indicates that the K_d for Ca^{2+} shows relatively little temperature dependence (53 μM at 37°C, 44 μM at 16.5°C). In contrast, furaptra's K_d for Mg^{2+} is more strongly temperature sensitive and in the opposite direction: 1.5 mM at 37°C vs. 5.3 mM at 16.5°C. A similar temperature sensitivity of fura-2's Ca^{2+} and Mg^{2+} K_d's has been reported (Grynkiewicz et al., 1985).

There are two possible discrepancies between the calibrations of Raju et al. (1989) and our own. Raju et al. report that the quantum efficiency of furaptra, when excited at 335 nm, is 25% larger in the Mg^{2+}-bound state compared with the metal-free state. In contrast, our calibrations (30 μM furaptra; excitation wavelength, 420 ± 15 nm; emission wavelengths, >495 nm) revealed that furaptra's fluorescence intensity per unit absorbance was essentially the same (within ±5%) at all levels of free [Mg^{2+}]. We have thus made no correction for differences in relative quantum efficiency in calibrating the in vivo signals (next section). The second discrepancy concerns the value of $\epsilon_{MgD}(420)/\epsilon_D(420)$. Although this value was not explicitly given by Raju et al. (1989), their Figs. 2 *A* and 5 suggest a value in the range of 0.05–0.15, compared with our value of 0.22.

In Vivo Measurements

All experiments were carried out on intact single twitch fibers dissected from semitendinosus or iliofibularis muscles of cold-adapted (4°C) *Rana temporaria*. The general procedures for fiber preparation, dye injection, and recording of signals on the optical bench apparatus have been described (e.g., Baylor and Hollingworth, 1988, 1990).

The furaptra-related optical signals were measured by procedures identical to those described previously for fibers injected with fura-2 (Baylor and Hollingworth, 1988). For both absorbance and fluorescence measurements, the excitation wavelength was usually set with a 420 ± 15 nm ("wide-band") interference filter inserted between the tungsten-halogen light source and the preparation. For fluorescence, a longer wavelength "cut-on" filter (OG 495; Schott Glass Technologies Inc., Duryea, PA), which passed light of wavelengths >495 nm, was inserted in the light path between the preparation and the photo-detector. The furaptra signals measured included the fluorescence intensity in the resting state (*F*), and the change in fluorescence intensity (ΔF) and absorbance (ΔA) as a result of action potential stimulation. The furaptra-related ΔA was obtained from the measured total absorbance change at 420 nm after subtraction of the estimated contribution from the intrinsic absorbance change of the fiber (denoted by $\Delta A_i(420)$). $\Delta A_i(420)$ itself was estimated by scaling $\Delta A_i(486)$, the intrinsic change measured at 486 nm (a wavelength where furaptra's absorbance is negligible), by the factor $(486/420)^{1.6}$ (cf. Hollingworth and Baylor, 1990).

Although the amplitudes of the ΔA and ΔF signals from furaptra are not maximized by the

use of a tungsten-halogen light source and a 420-nm excitation beam (cf. Fig. 1), the signals measured were in most cases well resolved in a single sweep. Moreover, there were some advantages to the use of 420-nm excitation (cf. Baylor and Hollingworth, 1988): (*a*) there was no contribution to F or ΔF from fiber intrinsic fluorescence; (*b*) since Ca^{2+}-bound furaptra has only 4% of the absorbance of Ca^{2+}-free furaptra, F and ΔF arose nearly exclusively from Ca^{2+}-free furaptra and changes in Ca^{2+}-free furaptra, respectively; and (*c*) nonlinearities due to the "inner filter effect" (see below) were generally small.

From the measured values of F, ΔF, and ΔA, estimates were obtained for the change in concentration of Ca^{2+}-furaptra complex (Δ[CaD]), the change in the myoplasmic free Ca^{2+} concentration ($\Delta[Ca^{2+}]$), and the total myoplasmic concentration of furaptra ($[D_T]$). The estimate of $\Delta[Ca^{2+}]$ does not depend on the ΔA measurement per se, whereas the indicator concentration estimates do depend on ΔA. For these conversions, the procedures used were similar to those described in Baylor and Hollingworth (1988), but included a few modifications.

Δ[CaD] was calculated from Beer's law:

$$\Delta A = \Delta\epsilon_{eff} \cdot \Delta[\mathrm{CaD}] \cdot l \tag{1}$$

where l denotes the optical length in myoplasm. $\Delta\epsilon_{eff}$, the change in effective extinction coefficient of furaptra upon complexation with Ca^{2+}, was calculated from:

$$\Delta\epsilon_{eff} = [\epsilon_{CaD} - (1 - f_{MgD}) \cdot \epsilon_D - f_{MgD} \cdot \epsilon_{MgD}] \tag{2}$$

In Eq. 2, ϵ_{CaD}, ϵ_{MgD}, and ϵ_D refer to the in vitro absolute extinction coefficients of furaptra in the Ca^{2+}-bound, Mg^{2+}-bound, and metal-free forms, respectively; in contrast, f_{MgD} refers to a property of the indicator in vivo; namely, the fraction of the indicator in the Mg^{2+}-bound form in the resting state. As described in the next paragraph, f_{MgD} was assumed to be 0.1. Eq. 2 also assumes that f_{CaD}, the fraction of the indicator in the Ca^{2+}-bound form in the resting fiber, is zero. This assumption is reasonable if furaptra does not enter the sarcoplasmic reticulum, since the K_d of furaptra for Ca^{2+} found in the in vitro calibrations is $\sim 10^3$ times larger than myoplasmic resting $[Ca^{2+}]$. $\Delta\epsilon_{eff}(420)$, calculated from Eq. 2 with the values of the extinction coefficients given in the preceding section, is 4.11×10^{-3} M^{-1} cm^{-1}.

Because of the limitations inherent in the use of a tungsten-halogen light source, information about the properties of furaptra at wavelengths <420 nm was not obtained in the muscle experiments; thus, it was not possible to accurately determine f_{MgD} experimentally. From the value 5.3 mM determined in vitro for $K_{d,Mg}$ (furaptra's K_d for Mg^{2+}) and from recent estimates from the literature for myoplasmic free $[Mg^{2+}]$ in frog muscle (0.8–2 mM; Alvarez-Leefmans et al., 1986; Baylor et al., 1986; Blatter et al., 1990), a first estimate is that f_{MgD} ($= [Mg^{2+}]/([Mg^{2+}] + K_{d,Mg})$) should be in the range 0.1–0.3. On the other hand, if, because of indicator binding to myoplasmic constituents (see Results and Discussion), the effective value of $K_{d,Mg}$ in vivo were >5.3 mM, f_{MgD} would be correspondingly smaller; for example, if the effective $K_{d,Mg}$ were twice the in vitro value, f_{MgD} should fall in the range 0.05–0.15. For the calibration of the Ca^{2+} transients detected from furaptra, we have assumed that $f_{MgD} = 0.1$; this corresponds to the assumption that myoplasmic free $[Mg^{2+}]$ was 0.11 times the effective $K_{d,Mg}$ in vivo.

Eq. 2 also assumes that [MgD] (the concentration of indicator in the fiber in the Mg^{2+}-bound form) divided by $[D]$ (the concentration of indicator in the metal-free form) remains constant during fiber activity. A constant [MgD]/$[D]$ ratio is expected if (*a*) the fractional change in myoplasmic free $[Mg^{2+}]$ is negligible during activity, and (*b*) the kinetics of the Mg^{2+}-furaptra reaction are rapid relative to the time course of Δ[CaD]. In fact, $[Mg^{2+}]$ is thought to remain nearly constant in response to a single action potential (Baylor et al., 1982*a*, *b*, 1985*b*; Irving et al., 1989; see also Results). The question of the reaction kinetics of the indicator with Mg^{2+} will be considered in the Discussion.

$\Delta[Ca^{2+}]$ was estimated from the measurements of F and ΔF by the following equations:

$$\Delta f_{CaD} = (\Delta F/F) \cdot (F/\Delta F_{max}) \quad (3)$$

$$\Delta[Ca^{2+}] = K_{d,eff} \cdot \Delta f_{CaD}/(1 - \Delta f_{CaD}). \quad (4)$$

In Eq. 3, Δf_{CaD} denotes the fraction of the indicator that is driven into the Ca^{2+}-bound form during fiber activity, $\Delta F/F$ is the change in fluorescence observed during activity divided by the resting fluorescence, and ΔF_{max} denotes the change in fluorescence that would be observed if all the indicator were to change to the Ca^{2+}-bound form. The use of Eqs. 3 and 4 assumes that f_{CaD} is zero (cf. above).

$\Delta F/F$ was measured in vivo in each experiment, whereas $F/\Delta F_{max}$ was estimated from the effective extinction coefficients assumed to apply to the indicator in the resting state, $(1 - f_{MgD})\cdot\epsilon_D + f_{MgD}\cdot\epsilon_{MgD}$ (to which F is proportional), and in the Ca^{2+}-bound state, ϵ_{CaD} (to which F-ΔF_{max} is proportional). From the values of the extinction coefficients determined in the in vitro calibrations, and the value assumed for f_{MgD}, 0.1 (see above), $F/\Delta F_{max}$ is calculated to be -1.045, the value used throughout Results. The value of $F/\Delta F_{max}$ was also checked by means of indicator-filled glass capillaries mounted on the optical bench, with fluorescence measured as in the muscle experiments. The value so determined for $F/\Delta F_{max}$ agreed within 1% of the calculated value ($= -1.045$).

From Δf_{CaD}, $\Delta[Ca^{2+}]$ was calculated by means of Eq. 4. $K_{d,eff}$ was assumed to be 48.9 μM (=44 μM/$(1 - f_{MgD})$), the value expected if Ca^{2+} and Mg^{2+} compete for the same binding site on the indicator and if the actual K_d of the indicator for Ca^{2+} is the same in myoplasm as measured in the in vitro calibrations (but see Discussion). From the above estimates of Δ[CaD] and Δf_{CaD}, $[D_T]$ was estimated from:

$$[D_T] = \Delta[CaD]/\Delta f_{CaD} \quad (5)$$

No attempt was made to estimate $[D_T]$ from the resting fluorescence measurement alone.

Empirical corrections to ΔA. As described in Baylor and Hollingworth (1988), two empirical corrections to the raw ΔA(420) measurement were required before application of Eq. 1. First, since the optical bench apparatus used high numerical-aperture condensing and collecting objectives (model 1509109; E. Leitz, Inc., Rockleigh, NJ: 32×; 0.6 NA), some contribution to the nominal change in 420 nm transmitted light intensity (ΔI) actually arose from a change in fluorescent light (ΔF) of longer wavelengths (a fraction of which, due to the high numerical aperture of the objective, is also collected and contributes to the measured ΔI). This ΔF reduced the amplitude of the intensity change that would have been measured at the incident wavelength (420 nm) due to the absorbance change alone. The factor required to correct for this effect was evaluated by the method described previously for fura-2 (Baylor and Hollingworth, 1988) and, in the case of furaptra, measurements on three fibers yielded an average value of 1.054 (±0.004, SEM). Second, to increase the signal-to-noise ratio, ΔA was usually measured with the wide-band, 420-nm filter (rather than a narrow-band filter). The use of the wide-band filter, however, implies that the effective extinction coefficient calculated in Eq. 2 involves some error. To correct for this error, raw ΔA's (i.e., uncorrected for the ΔF contribution to ΔI) were measured close in time, and in a bracketed fashion, first with the wide-band and then the narrow-band (420 ± 5 nm) filter. The ratio of ΔA(420, narrow-band)/ΔA(420, wide-band) so determined in three fibers was 1.090 (±0.011, SEM). Thus, to correct for both effects described in this paragraph, the raw measurements of ΔA(420, wide-band) were multiplied by 1.149 (=1.090 × 1.054) before use of Eq. 1.

Corrections for the inner filter effect. With 420-nm excitation the absorbance of the incident light by furaptra was usually small (cf. Fig. 1) but not always entirely negligible. (Note, however, that furaptra's absorbance of its own fluorescence, which is emitted primarily at wavelengths

longer than 450 nm, is negligible; Raju et al., 1989; our own measurements). As an example, a 1-mM concentration of furaptra in a 100-μm-diam fiber (for which the optical path length in myoplasm is ~70 μm (Baylor et al., 1983*a*) should, according to Beer's law, increase the fiber's resting absorbance of 420-nm light by ~0.024 if averaged over the full diameter of the fiber (cf. Baylor et al., 1986). This absorbance would increase to ~0.030 if furaptra's absorbance over a 405–435-nm band-width (the approximate band-width of our 420-nm, wide-band filter) were considered (cf. Fig. 1). An absorbance of 0.030, in turn, implies that only 0.933 ($=10^{-0.030}$) of the excitation beam incident on the fiber is actually transmitted by the fiber and available for fluorescence excitation at the far side of the fiber. Thus, the relationship between indicator concentration and indicator fluorescence becomes nonlinear at higher indicator concentrations ("inner filter effect;" Cantor and Schimmel, 1980). One consequence of this effect is that the value of Δf_{CaD} calculated by means of Eq. 3 is underestimated.

To correct for the nonlinearity between indicator concentration and fluorescence, Eq. 5′ of Baylor et al. (1981) was used. The accuracy of the correction was checked empirically under in vitro conditions by measurements with quartz capillaries (inner diameter, 150 μm) that contained furaptra at concentrations as high as 2.2 mM and was found to be very close (±2%) to the theoretically calculated correction. Although corrections for the inner filter effect were usually small (<5%), they have been applied routinely throughout Results. For example, with 1 mM indicator, the effect of the correction on a Δf_{CaD} between 0.07 and 0.14 (the range usually encountered in the muscle experiments) was to increase Δf_{CaD} by factors of 1.033 and 1.030, respectively.

Measurements with polarized light. As in previous work (e.g., Baylor and Hollingworth, 1988), the absorbance measurements were routinely made with two forms of polarized light, denoted by 0° and 90°, referring, respectively, to light polarized parallel and perpendicular to the long axis of the fiber. For this purpose, fibers were illuminated with unpolarized light, and a polarizing beam-splitting prism (Karl Lambrecht Corp., Chicago, IL) positioned in the light path after the muscle fiber diverted the 0° and 90° transmitted light to two identical photo-detectors, which measured the respective resting intensities (denoted by I_0 and I_{90}) and changes in intensities during fiber activity (denoted by ΔI_0 and ΔI_{90}).

In a few experiments the fluorescence emission anisotropy (denoted by A) of furaptra was measured and analyzed under both in vitro and in vivo conditions, as previously described for fura-2 (Konishi et al., 1988). For this purpose, indicator fluorescence was excited with 0° (or 90°) linearly polarized light by means of a crystal polarizer positioned between the light source and the preparation, and the intensity of the fluorescent light polarized parallel ($F_\parallel$) and perpendicular ($F_\perp$) to the excitation beam was measured. Anisotropy was calculated from the equation:

$$A = \frac{F_\parallel - F_\perp}{F_\parallel + 2F_\perp} \tag{6}$$

(Cantor and Schimmel, 1980).

As described in the preceding paper (Konishi and Baylor, 1991), intrinsic birefringence signals (denoted by ΔB) were measured both before and after injection of indicator as a means of assessing possible fiber damage associated with the injection. Except for one fiber (see note in legend of Table II), ΔB was not changed significantly as a result of the injection.

Measurement limitations. In principle, indicator-related absorbance and fluorescence levels might be measured from resting fibers injected with furaptra. However, at the usual myoplasmic concentrations of furaptra achieved in the experiments (<1.5 mM), indicator-related absorbance at 420 nm is expected to be less than the fiber's intrinsic absorbance at 420 nm (0.04–0.05); thus, resting absorbance signals from furaptra were not well resolved and are not reported in this paper. In contrast, resting fluorescence intensities from furaptra at myoplasmic

concentrations as small as 40–50 μM could be reliably resolved. The main limitation in resolving fluorescence intensities at smaller indicator concentrations arose from a non–dye-related component of intensity due to the non-zero overlap in the transmission band of the primary (420 ± 15 nm) and secondary (>495 nm) filters. The contribution of this component was estimated in all experiments and subtracted from the raw intensity measurements to obtain the indicator-related component (denoted by F).

RESULTS

Fluorescence Signals from Resting Fibers

Apparent diffusion constant of furaptra in myoplasm. To estimate the percentage of furaptra bound to myoplasmic constituents of large molecular weight, the indicator's

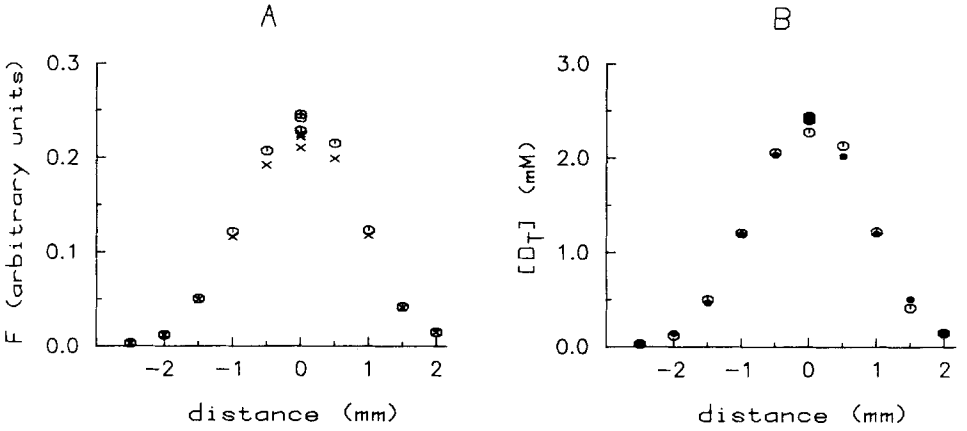

FIGURE 3. Estimation of furaptra's apparent diffusion constant in myoplasm and the total quantity of indicator within the fiber. (*A*) The crosses show furaptra's fluorescence intensity levels F (ordinate) measured at different distances (abscissa) along the fiber axis from the dye injection site (0 mm). The open circles show the values of F after correction for the inner filter effect (see text). (*B*) The open circle data are the same as in *A*, except the scale on the ordinate has been calibrated in terms of total furaptra concentration, $[D_T]$. The small filled circles show the values of $[D_T]$ predicted from Eq. 7 after least-squares adjustment of the parameters D_{app} and M. The fitted values were 0.77×10^{-6} cm^2 s^{-1} and 0.511 μmol cm^{-2}, respectively. Fiber reference, 112289.1; sarcomere length, 3.8 μm; fiber diameter, 101 μm; 16.0°C; 76–79 min after injection. For each of the measurements shown in *A*, the full fiber diameter and an 87-μm length of fiber was illuminated with a 420 (±15)-nm excitation beam.

apparent diffusion constant in myoplasm, D_{app}, was estimated from resting fluorescence levels measured at different distances from the site of dye injection. The general procedure was similar to that described for fura-2 (Baylor and Hollingworth, 1988; see also Konishi and Baylor, 1991), but included the additional correction for the inner filter effect as described in Methods.

Fig. 3 shows an example of the measurements and analysis, as applied to a fiber in which the furaptra concentrations along the fiber axis varied between 0 and 2.4 mM at the time of the measurements (76–79 min after injection). The crosses in Fig. 3 *A*

show the raw measurements of the resting fluorescence intensities; the open circles show the data after correction for the inner filter effect. The corrected data, after conversion to concentration units (see Methods), have been replotted as the open circles in Fig. 3 *B*.

To estimate the parameters D_{app} ($cm^2\ s^{-1}$) and a second parameter M ($\mu mol\ cm^{-2}$; proportional to the total quantity of indicator contained within the fiber), the data in Fig. 3 *B* were least-squares fitted by the solution of the one-dimensional diffusion equation (Crank, 1956):

$$[D_T](x, t) = \frac{M}{2\sqrt{\pi D_{app} t}} \exp\left(-x^2/(4D_{app}t)\right) \quad (7)$$

where $[D_T]$ (x,t) denotes indicator concentration at distance x from the injection site and time t after injection. The filled circles in Fig. 3 *B* show the results of the fit, which yielded the estimates of M and D_{app} given in the legend of Fig. 3.

Table I shows values of D_{app} similarly estimated in six fibers; in four of the six fibers, several estimates were obtained at different times after injection. The mean value (±SEM) estimated ~40–80 min after injection was 0.68 (±0.02) × 10^{-6} $cm^2\ s^{-1}$. For a molecule the size of furaptra (mol wt 430 for the tetra-valent form), the true diffusion constant in myoplasm, i.e., that which would be measured in the absence of binding, is expected to be ~1.2–1.4 × 10^{-6} $cm^2\ s^{-1}$ at 16°C (cf. Kushmerick and Podolsky, 1969; Maylie et al., 1987*a*, *b*). Thus, the average value of D_{app} for furaptra, 0.68 × 10^{-6} $cm^2\ s^{-1}$, suggests that 42–51% of the indicator was bound to myoplasmic constituents of low mobility (cf. Eq. 3 of Konishi and Baylor [1991] and associated discussion).

Because of the initial spread of the indicator during the pressure injection, fits to diffusion measurements made relatively early after injection (e.g., <30 min) will overestimate the value of D_{app}. (In contrast, the value of M should not be in error, since, according to Eq. 7, the value of M is independent of errors in time.) This effect on D_{app} becomes negligible at measurement times later than ~30 min after injection (cf. Baylor et al., 1986); thus, the average value of D_{app} mentioned in the preceding paragraph was obtained from measurements between 40 and 80 min after injection. It may be noted, however, that even with exclusion of measurements obtained at times earlier than 30 min after injection, the data in Table I for any particular fiber reveal a decrease in the estimates of D_{app} with time. Thus, this decrease is probably a genuine property of furaptra's diffusion in myoplasm. A decrease in the estimate of D_{app} with time after injection was reported previously for antipyrylazo III (Baylor et al., 1986) and may also apply to tetramethylmurexide (TMX) and PDAA (see Table I of Konishi and Baylor [1991] and associated discussion).

Time-dependent changes in the parameter M. For each of the four fibers in Table I for which D_{app} and M were estimated at significantly different times, smaller values of M were also observed at later times after injection. A similar effect was also detected in fibers injected with TMX and PDAA (Konishi and Baylor, 1991), but was not seen with antipyrylazo III (Baylor et al., 1986), fura-2 (Baylor and Hollingworth, 1988), or phenol red (Baylor and Hollingworth, 1990).

Fig. 4 *A* plots the relative value of M observed in two experiments (*crosses and open circles*) as a function of time t after furaptra injection. The data from each experiment

have been fitted by the functional form $M(t)/M(0) = \exp(-t/\tau)$, where $M(0)$ denotes the value of M at the time of injection and τ denotes the time constant for decay of M. For the two experiments in Fig. 4 *A*, the fitted values of τ (112 and 733 min) represent the extremes of the range of values seen in the four experiments (cf. column *6* of Table I), all of which revealed clear evidence for a time-dependent decrease in M.

TABLE I

Estimation of the Apparent Diffusion Constant (and Related Parameters) of Furaptra in Intact Muscle Fibers

Fiber	Time	Average $[D_T]$ at injection site	D_{app}	M	τ
	min	*mM*	10^{-6} *cm^2 s^{-1}*	*μmol cm^{-2}*	*min*
(*1*)	(*2*)	(*3*)	(*4*)	(*5*)	(*6*)
030389.3	67–72	1.347	0.68	0.263	—
112089.1	8–12	0.322	(0.74)	0.026	146
	55–63	0.112	0.68	0.020	
	118–124	0.049	0.62	0.012	
112089.2	45–47	0.062	0.64	0.009	—
112089.3	23–25	0.364	(0.71)	0.042	216
	98–102	0.137	0.61	0.029	
112289.1	10–14	5.199	(1.33)	0.568	733
	25–29	3.864	(0.90)	0.527	
	76–79	2.358	0.77	0.511	
	83–86	2.236	0.74	0.499	
	148–151	1.600	0.65	0.449	
	261–263	1.150	0.57	0.397	
112289.2	15–21	0.232	(0.66)	0.022	112
	57–61	0.099	0.64	0.017	
	104–108	0.053	0.52	0.011	
	143–146	0.034	0.43	0.007	
Mean (± SEM)			0.68* (± 0.02)		302 (± 145)

The table is based on least-squares fits of Eq. 7 to the furaptra concentration data measured at different times after injection and distances from the injection site; for each run, 6–11 measurements of $[D_T]$ were made (cf. Fig. 3). Column *1* gives the fiber identification; column *2*, the times after injection; column *3*, the average indicator concentration measured at the injection site during the run; columns *4* and *5* show the fitted values of the parameters in Eq. 7: D_{app} (the apparent diffusion constant) and M (proportional to the total amount of furaptra injected into the fiber). Column *6* gives, for fibers having more than one run, the least-squares estimate of τ, the time constant for decay of the value of M (cf. text and Fig. 4 *A*). *Each fiber contributed one value to the calculation of mean and SEM; the value of D_{app} used for each fiber was that estimated between 40 and 80 min after injection. In column *4* the values of D_{app} within parentheses are probably artifactually high because of the early measurement times (<30 min) after injection (see text). Sarcomere lengths, 3.6–3.9 μm; fiber diameters, 88–105 μm; 15.9–16.2°C.

Three possibilities may be proposed to explain the decline in M with time after injection: (*a*) the indicator leaves the cell (as is the most likely explanation for the decrease in M observed with the purpurate indicators; cf. Konishi and Baylor, 1991);

(*b*) the indicator enters a high Ca^{2+} environment within the fiber such as the sarcoplasmic reticulum (where most of the furaptra would exist in a very weakly fluorescent Ca^{2+}-bound state); or (*c*) the indicator is metabolized or chemically altered in such a way as to become much less fluorescent. (The latter possibility, if correct, is not attributable to a photo-bleaching of furaptra, however. Several in vivo measurements were made of the reduction in furaptra's fluorescence as a result of a prolonged (2–4 min) period of excitation with the 420-nm beam, which illuminated a fiber length of 300 μm. Photo-bleaching was then evaluated by fluorescence measure-

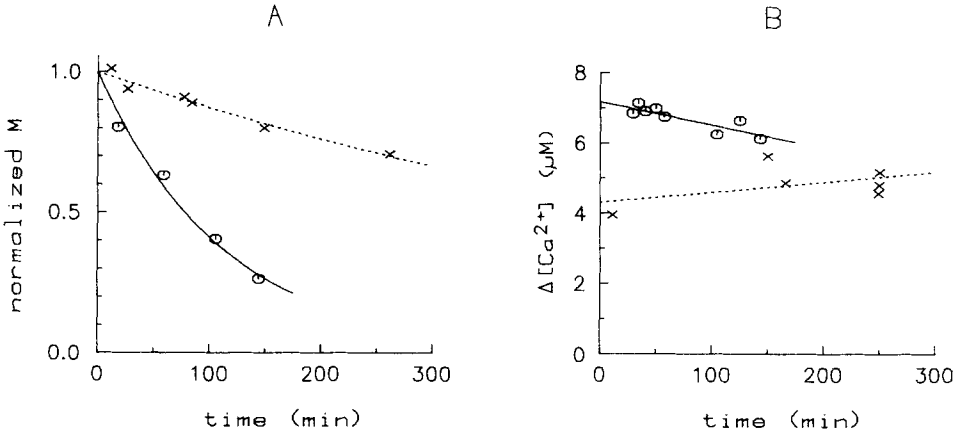

FIGURE 4. (*A*) Examples from two fibers showing the relative variation in the parameter M in Eq. 7, as obtained from fits of the type shown in Fig. 3 *B* and summarized in columns *4* and *5* of Table I, plotted as a function of time t after dye injection. For any one fiber, the set of values of M were least-squares fitted by the functional form: $M(t) = M(0) \cdot \exp(-t/\tau)$, where $M(0)$ denotes the estimated value of M at the time of injection. Plotted in the figure are the values of $M/M(0)$, along with the curve $\exp(-t/\tau)$. Crosses are from fiber 112289.1; sarcomere length, 3.8 μm; fiber diameter, 101 μm; 16.0°C; fitted value of τ, 733.1 min. Open circles are from fiber 112289.2; sarcomere length. 3.8 μm; fiber diameter, 92 μm; 16.1°C; τ, 112.4 min. (*B*) Variation with time after injection (abscissa) of the peak value of the myoplasmic Ca^{2+} transient (ordinate) as calibrated from furaptra's $\Delta F/F$ signal measured in response to a single action potential. The data (*open circles and crosses*) are from the same two experiments as shown in *A*. Only measurements from fiber regions containing furaptra at nonbuffering concentrations have been included in the plot (range of indicator concentrations: 0.15–0.52 mM [112289.1], 0.04–0.16 mM [112289.2]). Each data set has been least-squares fitted with a straight line.

ments with a 70-μm vertical slit of 420-nm light positioned in the middle of the originally illuminated field, i.e., so that the measurements would not be confounded by a rapid diffusion of indicator back into the 300-μm field. The amount of photo-bleaching was small, less than 1/40 of the amount required to explain the typical decreases in M observed for the measurements in Table I).

For three of the four fibers in Table I the fitted values of τ were relatively small (112, 146, and 216 min), whereas the fourth value (733 min) was measured from the fiber that had by far the largest concentration of injected indicator (>5 mM measured at the injection site 10–14 min after injection; cf. columns *3* and *5* of Table

I). This observation suggests that the mechanism whereby indicator leaves the myoplasm (or is modified within the myoplasm) might involve a saturable transport system (or a metabolic pathway with saturable reaction rates). If the fiber with the very large furaptra concentration is excluded, the average value (±SEM) of τ was 158 ± 31 min, which is intermediate between the values of τ observed with TMX (46 ± 7 min) and with PDAA (338 ± 82 min) (Konishi and Baylor, 1991).

Fluorescence emission anisotropy. In the case of a fluorescence indicator, a comparison of in vitro and in vivo anisotropy levels (denoted by A) provides another way to evaluate the degree of binding of indicator to relatively immobile fiber constituents (Konishi et al., 1988). In vivo, the average value of A in three fibers was 0.189 (±0.006) if measured with a 90° excitation beam and 0.182 (±0.005) if measured with 0° polarized light. The difference between the three pairs of values, 0.007 (±0.007), is not significantly different from zero, as expected if most of the furaptra molecules within the fiber are randomly oriented. The average value of all the measurements, 0.185 (±0.004), has been used to estimate the bound fraction of furaptra in myoplasm. For the latter purpose, furaptra's in vivo anisotropy was compared with that measured at 16°C in salt solutions of varying viscosity, 1.1–8.4 centipoise (cP), set by variable additions of sucrose (cf. Konishi et al., 1988). As expected, anisotropy varied monotonically with viscosity, from 0.06 at 1.1 cP to 0.24 at 8.4 cP. The average in vivo A value, 0.185, corresponds to a solution viscosity of ~4.8 cP. Since the viscosity of myoplasm is probably close to 2 cP (Kushmerick and Podolsky, 1969), the in vivo value is not consistent with all of the indicator being freely dissolved in myoplasm. Rather, it is likely that myoplasmic A is elevated because a significant fraction of furaptra is bound to relatively immobile sites. Since fura-2's in vivo anisotropy corresponded to a solution viscosity of 6.4 cP (Konishi et al., 1988), the percentage of bound furaptra appears to be somewhat less than the 60–85% range estimated for fura-2 by three different methods (from measurements of D_{app} in vivo, from measurements of a blue shift in fura-2's in vivo emission spectrum, and from simultaneous in vitro measurements of anisotropy and fluorescence intensity). Thus, the furaptra anisotropy measurements are consistent with the inference from the D_{app} measurements described above, in which the percentage of bound furaptra was estimated to be 42–51%.

Furaptra Ca^{2+} Signals during Fiber Activity

In Fig. 5, the upper three traces show original optical records obtained in response to a single stimulated action potential, from a fiber region containing 0.79 mM furaptra. The upper two traces show the fractional change in transmitted light intensity at the wavelength indicated in nanometers to the left. The 486-nm record reflects the fiber intrinsic change alone, whereas the 420-nm record reflects this change plus a relatively large, early increase in transmitted intensity due to the presence of furaptra. The estimate of the indicator-related absorbance change at 420 nm is shown at the bottom of Fig. 5 (dotted trace, which has been calibrated in terms of the change in concentration of Ca^{2+}-indicator complex; cf. Methods). The third trace in Fig. 5 (labeled ΔF) shows the change in fluorescence from furaptra. This trace is also shown, with inverted polarity, at the bottom of the figure (continuous trace) and has a time course identical to that of the absorbance change.

The time course of the indicator-related change in Fig. 5 (time-to-peak, 7 ms; half-width, 12 ms) is similar to $\Delta[Ca^{2+}]$ previously recorded at this temperature in fibers injected with PDAA (Konishi and Baylor, 1991) or submillimolar concentrations of antipyrylazo III (Baylor and Hollingworth, 1988). If the $\Delta F/F$ signal in Fig. 5 is calibrated in terms of $\Delta[Ca^{2+}]$ by means of Eqs. 3 and 4, the peak amplitude is 4.1

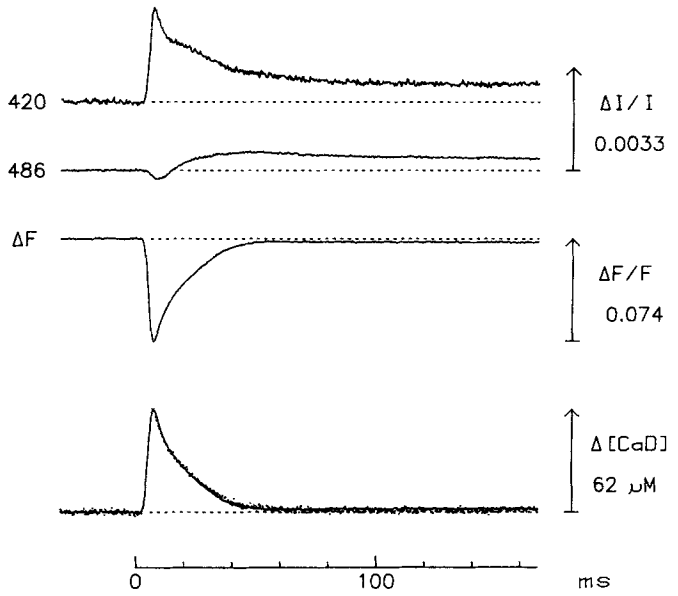

FIGURE 5. The upper three traces show original records of fiber transmission changes (obtained at 420 and 486 nm, as indicated) and the fluorescence change ΔF (420 ± 15-nm excitation, >495-nm emission), measured from a fiber containing 0.79 mM furaptra. At zero time the fiber was stimulated to give a single action potential. The superimposed pair of traces at the bottom compares the time courses of furaptra's absorbance changes (*dotted trace*) and fluorescence change (*continuous trace;* same as ΔF above, but with inverted polarity). The ΔA waveform was obtained from the 420-nm transmission record after subtraction of the 486-nm record scaled by the factor $(486/420)^{1.6}$. The calibration bar for Δ[CaD] was obtained from the peak of ΔA (−0.00144) after calibration by Beer's law under the assumption that ΔA arises entirely from the formation of Ca^{2+}-indicator complex (see Methods). The traces were recorded 1.5 mm from the dye injection site, 155–158 min after injection. The transmission measurements were made with a 73-μm spot of light, whereas the fluorescent light was collected from a 300-μm fiber length and the full fiber diameter. The 486-nm record is a single sweep, whereas the other traces are averages of two sweeps. Fiber no., 112289.1 (see legend of Fig. 4 for additional fiber information).

μM. If, additionally, the calibration is corrected for a calculated 2% underestimate of Δf_{CaD} due to the inner filter effect (see Methods), peak $\Delta[Ca^{2+}]$ becomes 4.2 μM.

Although the in vitro calibrations indicate that at 16–17°C furaptra's K_d for Ca^{2+} is 120 times smaller than that for Mg^{2+}, it is possible that $\Delta[Mg^{2+}]$ makes a contribution to the furaptra-related signals in Fig. 5. It is likely, however, that the contribution of

$\Delta[Mg^{2+}]$ is quite small, except at late times in the transient (cf. last two sections of Results). We have therefore routinely calibrated the furaptra signals in this paper in terms of $\Delta[Ca^{2+}]$ alone.

As a monitor of the myoplasmic Ca^{2+} transient, the ΔF signal has several advantages over the ΔA signal: (*a*) it can be recorded at a single wavelength, generally without requiring a correction for fiber intrinsic changes measured at a second wavelength; (*b*) it is less subject to interference from movement artifacts (which are not seen in Fig. 5 but are seen in some cases; e.g., the traces in Fig. 9 at shorter sarcomere length); (*c*) it can be directly calibrated in terms of $\Delta[Ca^{2+}]$, even at low indicator concentrations; (*d*) it has a somewhat larger signal-to-noise ratio (at least as recorded by our apparatus). On the other hand, the ΔA signal has the advantage that it can be directly calibrated in units of Δ[CaD], a measurement that gives information about the extent of buffering of the Ca^{2+} transient by the indicator (cf. Fig. 7 and associated discussion). The Δ[CaD] measurement, in combination with the $\Delta F/F$ measurement, also permits an estimate of the total indicator concentration in myoplasm, $[D_T]$ (cf. Eqs. 3–5).

Table II summarizes the properties of the furaptra $\Delta[Ca^{2+}]$ signal recorded from 16 fibers. The average kinetic parameters (columns *6* and *7*) are closely similar to those summarized in Table II of the preceding paper (Konishi and Baylor, 1991) for fibers injected with PDAA; however, the peak amplitude of $\Delta[Ca^{2+}]$, 5.1 (±0.3, SEM) μM, is approximately half that observed with PDAA. The average kinetic parameters are also closely similar to those of $\Delta[Ca^{2+}]$ recorded in fibers injected with antipyrylazo III (Baylor and Hollingworth, 1988); however, the average peak value of antipyrylazo III's $\Delta[Ca^{2+}]$ at 1.8 μM (±0.2, SEM) is ~2.8 times smaller than that of furaptra.

Simultaneous Comparison of $\Delta[Ca^{2+}]$ Signals from Furaptra and PDAA

To make a more precise comparison of the amplitude and time course of $\Delta[Ca^{2+}]$ estimated with furaptra and PDAA, two experiments were carried out on single fibers simultaneously injected with both indicators. The presence of furaptra, which has no absorbance at $\lambda \geq 450$ nm (cf. Fig. 1), is not expected to influence the $\Delta[Ca^{2+}]$ signal from PDAA, which is routinely recorded at $\lambda \geq 450$ nm. Conversely, the presence of PDAA at the concentrations used to measure its $\Delta[Ca^{2+}]$ in these experiments (1–1.3 mM), is expected to have a negligible effect on furaptra's $\Delta[Ca^{2+}]$. For example, at 420 nm PDAA's ΔA during activity is extremely small and its influence on furaptra's ΔF is calculated to be entirely negligible. On the other hand, for $\lambda > 495$ nm (the wavelength range used to measure furaptra's emitted fluorescence), PDAA's absorbance change is larger, but on average still small, <0.0005–0.001 ΔA units. Thus, the contribution of this change to the measurement of furaptra's $\Delta F/F$ signal, the peak value of which is in the range 0.06–0.11, is expected to be no more than 3%. No attempt was made to correct for this small error.

Fig. 6 shows optical signals recorded during activity from a region of a single fiber that contained both PDAA (at 1.25 mM) and furaptra (at 0.26 mM). *A* shows the transmission records used to estimate PDAA's $\Delta[Ca^{2+}]$ signal. The lowermost record (at 700 nm) was used to estimate and remove the contribution of the fiber intrinsic change from the upper two transmission records, which show estimates of the PDAA-related signal at the indicated wavelengths. The superimposed pair of traces in

TABLE II

Analysis of Signals Recorded in Response to a Single Action Potential in Fibers Injected with Furaptra

Fiber number	$[D_T]$	Time after injection	ΔB		$\Delta[Ca^{2+}]$			$\frac{\Delta F_{steady}}{\Delta F_{peak}}$
			Time to peak	Peak $\Delta I/I$	Time to peak	Half-width	Peak value	
	μM	*min*	*ms*	-10^{-3}	*ms*	*ms*	μM	
(1)	*(2)*	*(3)*	*(4)*	*(5)*	*(6)*	*(7)*	*(8)*	*(9)*
030389.3	212	71	8.4	1.5	7.1	7.3	5.1	+0.040
052589.2	366	4	8.8	1.8	6.4	12.1	5.6	+0.040
060689.4	133	6	—	—	6.4	9.3	4.4	+0.074
062289.3	137	6	8.4	1.3	6.9	10.8	4.8	—
062889.2	93	22	9.6	1.7	6.4	9.4	4.5	+0.037
062889.3	107	16	—	—	6.0	7.4	4.0	—
082989.2	236	8	—	—	6.2	7.3	4.2	—
112089.1	410	5–8	9.2	1.6	6.4	11.7	4.4	+0.068
112089.2	169	6	10.4	1.4	6.8	10.1	4.5	+0.054
112089.3	490	14	—	—	6.4	10.2	4.7	+0.047
112289.1	205	11	—	—	7.0	11.0	4.0	—
112289.2	162	32–35	9.2	2.1	6.4	10.4	6.8	+0.051
030890.1	288	18–21	—	—	6.2	8.4	7.7	—
030990.1	340	7	7.6	1.0	5.6	8.6	4.9	—
030890.2	90	10	9.6	3.0	5.0	9.2	6.6	—
031590.3	373	6–9	8.0	1.7	5.2	8.4	5.3	+0.063
Mean (± SEM)			8.9 (±0.3)	1.7 (±0.2)	6.3 (±0.1)	9.5 (±0.4)	5.1 (±0.3)	+0.053 (±0.004)

Column *1* gives the fiber reference; column *2*, the average furaptra concentration during the run; and column *3*, the time after injection during which the run was made. Columns *4* and *5* give information about the time to peak and peak value, respectively, of the intrinsic birefringence signal (ΔB) recorded at 700 nm during the run. The remaining columns refer to information obtained from $\Delta F/F$ measurements of the type shown in Fig. 5. Columns *6–8* give, respectively, the time-to-peak value, the half-width, and the peak change in myoplasmic free $[Ca^{2+}]$ if $\Delta F/F$ is converted to $\Delta[Ca^{2+}]$ by the calibration procedure described in Methods. Column *9* gives the value of ΔF averaged over the interval 128–168 ms after stimulation divided by the peak value of ΔF. For the 12 experiments, fiber diameters varied between 78 and 119 μm, and bath temperatures between 15.9 and 16.4°C. Each entry in the table is based on an average of one to two sweeps. For inclusion in the table, the earliest run from each fiber was selected for which $[D_T]$ was between 0.09 and 0.50 mM and sarcomere length was between 3.6 and 4.0 μm. A dashed entry indicates that a movement artifact made the measurement of the peak of the birefringence signal unreliable. Except for fiber 030389.3, the peak amplitude of the birefringence signal (or rate of rise of the signal if the measurement of peak amplitude was unreliable because of a movement artifact) was not changed significantly by the injection of indicator. For fiber 030389.3, the peak amplitude was reduced by 30% (without a change in time course); for the other fibers, the average change in ΔB amplitude was −3% (±2%, SEM) as a result of the injection. In column *9*, $\Delta F_{steady}/\Delta F_{peak}$ was estimated only for fibers that showed a monotonic decay of ΔF, i.e., for which contributions from movement artifacts were likely to have been small.

A (middle) shows a comparison of the time courses of the 542- and 486-nm signals from the indicator. As expected, these signals have an identical time course during the main phase of the PDAA transient (up to ~20 ms after stimulation); at later times the signals diverge, probably because of a contribution to both traces from a movement artifact.

In Fig. 6 *B* the upper pair of traces compares the time course of the furaptra

fluorescence signal (arrowed trace) with PDAA's "difference" absorbance signal, $\Delta A(486) - \Delta A(542)$. This difference record is presumed to have a smaller contamination from movement artifacts than either the $\Delta A(486)$ or $\Delta A(542)$ trace alone (cf. Konishi and Baylor, 1991). The upper pair of traces in Fig. 6 *B* have very similar rising phases and times to peak; however, the falling phase of furaptra's fluorescence change lags slightly behind that of PDAA's absorbance change. The pair of superimposed traces at the bottom of Fig. 6 *B* compares the time courses of $\Delta[Ca^{2+}]$

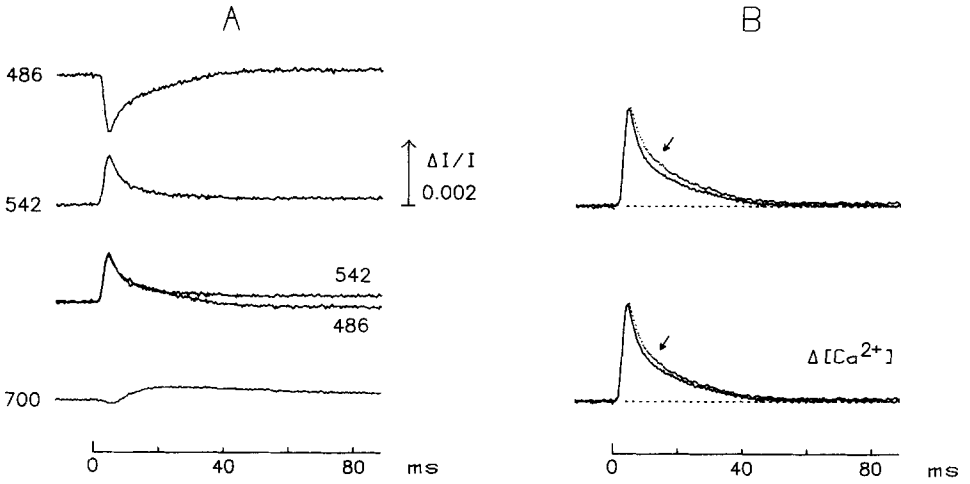

FIGURE 6. Comparison of time course of $\Delta[Ca^{2+}]$ as inferred from PDAA and furaptra in a fiber simultaneously injected with both indicators. (*A*) Transmission records at the wavelength indicated in nanometers to the left. The lowermost record (700 nm) reflects intrinsic changes alone. All other records are dye related; i.e., have been corrected for the intrinsic change by means of the 700-nm trace and the procedure described in Methods. The superimposed pair of traces shows the 542-nm trace (unscaled) and the 486-nm trace scaled by the factor −0.80. (*B*) Upper part shows a superposition of the furaptra ΔF signal (arrowed trace; peak value of $\Delta F/\Delta F_{max} = 0.119$) and the $\Delta A(486) - \Delta A(542)$ signal from PDAA (continuous trace; peak value of $\Delta A/\Delta A_{max} = 0.0096$). Lower part shows a superposition of the $\Delta[Ca^{2+}]$ signals scaled to have the same displayed peak amplitude. Peak values of $\Delta[Ca^{2+}]$ were 6.6 μM from furaptra (*arrowed trace*) and 8.5 μM from PDAA. Fiber reference, 030489.1; sarcomere length, 4.0 μm; 16.1°C; fiber diameter, 90 μm. Absorbance was measured with a 73-μm-diam spot; fluorescence was measured from the full fiber diameter and a 300-μm length. Total indicator concentrations were 1.25 mM (PDAA) and 0.26 mM (furaptra).

estimated from the two indicators. Less difference is seen between these traces and the upper pair of traces because the calculation of furaptra's $\Delta[Ca^{2+}]$ takes into account the (slight) nonlinearity in the relation between $\Delta F/F$ and $\Delta[Ca^{2+}]$. For the $\Delta[Ca^{2+}]$ traces, the times to peak and half-widths of the signals were 4.4 vs. 4.6 ms and 6.3 vs. 8.0 ms, respectively (PDAA vs. furaptra).

A very similar temporal relationship was also observed in the second fiber, which contained PDAA at 1.04 mM and furaptra at 1.19 mM. Although the amplitude of

$\Delta[Ca^{2+}]$ in this experiment was somewhat smaller than normal (see next paragraph), probably because of some fiber damage due to injection of the indicators, nevertheless a comparison of time courses of $\Delta[Ca^{2+}]$ as recorded with the two indicators should still be meaningful. In this experiment, the times to peak and half-widths of $\Delta[Ca^{2+}]$ were 6.0 vs. 6.4 ms and 10.7 vs. 12.2 ms, respectively (PDAA vs. furaptra). The slightly greater half-widths estimated for $\Delta[Ca^{2+}]$ in this experiment compared with that of Fig. 6 may, at least in part, be due to the use of furaptra at a slightly "buffering" concentration (1.19 mM; cf. Fig. 7 *B* and related discussion below).

For the experiments that involved a single indicator, the average value of the peak amplitude of $\Delta[Ca^{2+}]$ recorded with PDAA was 1.8 times that recorded with furaptra. A somewhat smaller difference was seen in the two simultaneous indicator experiments just described; in these experiments, peak $\Delta[Ca^{2+}]$ estimated from PDAA was only 1.29 and 1.31 times that estimated from furaptra (8.5 vs. 6.6 μM and 4.5 vs. 3.5 μM, respectively). Although the reason for this difference (1.8- vs. 1.3-fold) is not known, two possibilities may be proposed. First, the average value of $\Delta[Ca^{2+}]$ may have been somewhat smaller for the fibers injected with furaptra than those injected with PDAA. Second, there might be some in vivo interaction between the two indicators (mediated, for example, by a common binding site) that alters the effective K_d for Ca^{2+} of one (or both) of the indicators.

The main conclusion from these simultaneous-injection experiments is that the time courses of $\Delta[Ca^{2+}]$ as estimated with PDAA and furaptra are extremely similar, although there may be a small delay, 1–2 ms, in the half-width of $\Delta[Ca^{2+}]$ estimated from furaptra. A slight increase in half-width but not in time to peak is also suggested by the average results in Table II of the preceding paper (Konishi and Baylor, 1991) compared with Table II of this paper: 8.7 (±0.5) vs. 9.4 (±0.4) ms for half-width and 6.5 (±0.3) vs. 6.3 (±0.1) ms for time to peak (PDAA vs. furaptra). An increased half-width for furaptra's $\Delta[Ca^{2+}]$ is not certain, however, as the fractionally smaller ΔA signal from PDAA could be slightly contaminated by contributions from an improperly corrected intrinsic change or movement artifact.

Simultaneous Comparison of $\Delta[Ca^{2+}]$ Signals from Furaptra and Antipyrylazo III

Experiments similar to those just described were also carried out on three fibers simultaneously injected with furaptra ($[D_T]$, 0.25–0.55 mM) and antipyrylazo III ($[D_T]$, 0.24–0.75 mM). An example of the records from one of the fibers has been published previously in abstract form (Baylor et al., 1989). The purpose of this section is to summarize the average results from the three fibers.

The Ca^{2+}-related antipyrylazo III signal was estimated in the usual way (Baylor et al., 1985*b*; Baylor and Hollingworth, 1988) from dye-related absorbance changes measured at 550, 660, and 720 nm, wavelengths at which furaptra has no absorbance. Thus, furaptra should not interfere optically in the measurement of the Ca^{2+}–antipyrylazo III signal. Moreover, as described above for PDAA, optical contributions from antipyrylazo III's ΔA at the wavelengths used to detect furaptra's $\Delta[Ca^{2+}]$ signal are very minor. At 420 nm the contribution from antipyrylazo III's ΔA is entirely negligible (cf. Baylor et al., 1985*b*), whereas at the wavelengths used to detect furaptra's emitted fluorescence ($\lambda > 495$ nm), contributions due to antipyry-

lazo III's ΔA are estimated to be no more than 1–4% of the measured ΔF in these experiments. Again, no attempt was made to correct for this small error.

In the three experiments, the average values of the times to peak and half-widths for $\Delta[Ca^{2+}]$ were 5.4 (±0.1) vs. 6.0 (±0.1) ms and 9.4 (±1.5) vs. 9.3 (±1.2) ms, respectively (antipyrylazo III vs. furaptra). Thus, as was reported above for PDAA, the time course of $\Delta[Ca^{2+}]$ measured with antipyrylazo III (which includes a correction for a 1.4-ms kinetic delay; Baylor et al., 1985*a*; cf. Maylie et al., 1987*a*) is not distinguishably different from that measured simultaneously with furaptra. However, as expected from the experiments on fibers injected with either anytipyrylazo III alone (Baylor and Hollingworth, 1988) or furaptra alone (Table II), there was a significant difference in the calibrated peak amplitude of $\Delta[Ca^{2+}]$. For the three fibers that contained both antipyrylazo III and furaptra, the average peak amplitude of $\Delta[Ca^{2+}]$ was 1.9 (±0.2) μM and 5.2 (±0.2) μM, respectively. These amplitudes differ by 2.7-fold, the factor expected from the experiments involving each indicator alone.

The finding that the time course of furaptra's $\Delta[Ca^{2+}]$ is extremely similar to that recorded simultaneously with either PDAA or antipyrylazo III supports the interpretation that the furaptra signal primarily reflects a rapid kinetic response to $\Delta[Ca^{2+}]$, with little or no interference from other myoplasmic events such as a change in free $[Mg^{2+}]$.

Does Furaptra's $\Delta[Ca^{2+}]$ Change with Time after Injection?

The measurements illustrated in Fig. 4 *A* and summarized in Table I, columns *5* and *6* indicate that furaptra either leaves the fiber, becomes sequestered within an internal compartment, or becomes chemically altered within the myoplasm as a function of time after injection. The latter two possibilities might, in turn, be associated with an artifactual alteration in $\Delta[Ca^{2+}]$ as reported by furaptra. It was therefore of interest to compare the properties of $\Delta[Ca^{2+}]$ measured within a single fiber at different times after injection.

Fig. 4 *B* plots the peak amplitude of $\Delta[Ca^{2+}]$ vs. time after injection, for the same two experiments shown in Fig. 4 *A*. The experimental data from each fiber (open circles and crosses) have been least-squares fitted by straight lines. The slopes of the lines, if normalized by the value of the *y* intercepts, correspond to changes of −5.4%/h and +4.1%/h (open circles and crosses, respectively). The analogous rates estimated in the two other experiments of Table I were −0.9%/h and −12.1%/h. The four experiments together indicate that there is little or no change in the amplitude of furaptra's $\Delta[Ca^{2+}]$ with time after injection. A similar absence of effect was also observed for the time to peak and half-width of $\Delta[Ca^{2+}]$ if plotted as a function of time after injection (not shown). Thus, whatever process accounts for the time-dependent change in *M* (Fig. 4 *A* and Table I) does not appear to be associated with a prominent change in the estimate of $\Delta[Ca^{2+}]$.

Furaptra's $\Delta[Ca^{2+}]$ Signal vs. Indicator Concentration

Another basic question about the furaptra signal concerns possible variations in $\Delta[Ca^{2+}]$ as a function of the indicator's concentration in myoplasm. Fig. 7, which summarizes information from four fibers, plots the peak amplitude (*A*) and half-width (*B*) of $\Delta[Ca^{2+}]$ as a function of $[D_T]$. The data suggest that there is little or no variation

in either variable with values of $[D_T]$ up to 0.5 mM. Above 0.5 mM the plots suggest that there is a decrease in peak amplitude and an increase in half-width with increasing $[D_T]$. These changes appear to be larger than any small differences expected simply on the basis of the different times of the measurements (cf. legend of Fig. 7 and preceding section). In fibers injected with fura-2, more dramatic effects of indicator concentration on the peak of $\Delta[Ca^{2+}]$ and a qualitatively different effect on the half-width of $\Delta[Ca^{2+}]$ were observed and were also attributed to the Ca^{2+}-buffering effects of the indicator (Baylor and Hollingworth, 1988). (The decrease rather than increase in half-width of $\Delta[Ca^{2+}]$ seen with larger fura-2 concentrations is explained by the slow "off" rate constant for the Ca^{2+}–fura-2 reaction.) With furaptra, the onset of the buffering effect is observed when peak Δ[CaD] becomes larger than

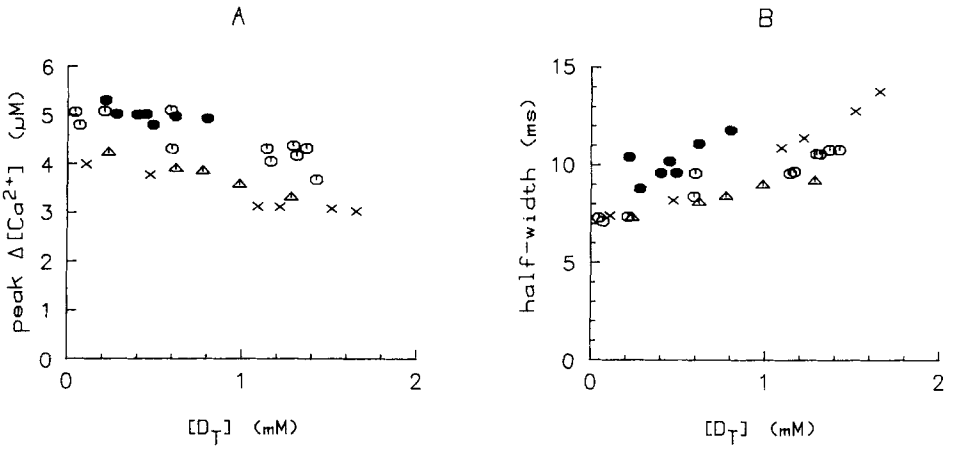

FIGURE 7. Dependence of properties of the myoplasmic Ca^{2+} transient measured with furaptra (*A*, peak value of $\Delta[Ca^{2+}]$; *B*, half-width of $\Delta[Ca^{2+}]$) on the total furaptra concentration in myoplasm ($[D_T]$). Fiber references: 030389.3 (*open circles*), 062889.3 (*crosses*), 082989.2 (*triangles*), 112089.3 (*filled circles*). Sarcomere lengths, 3.6–3.9 μm; fiber diameters, 78–105 μm; 16.0–16.4°C. Within any one experiment, measurements were made at different distances (up to 2 mm) from the injection site and different times (up to 72 min) after dye injection (2–70 min, *open circles;* 1–23 min, *crosses;* 1–11 min, *triangles;* 2–15 min, *filled circles*), thus accounting for the range of values observed for $[D_T]$.

~40–50 μM ($[D_T] \geq 0.5$ mM, in combination with a peak Δf_{CaD} ~0.09). This concentration range is somewhat smaller than the 60–80-μM range observed previously with fura-2; however, a smaller value is to be expected for furaptra since the time-to-peak of its Δ[CaD] signal (6–7 ms) is earlier than that of fura-2 (15–20 ms). In contrast to the effects observed in Fig. 7, no significant difference was detected in the time to peak of $\Delta[Ca^{2+}]$ if plotted as a function of $[D_T]$ (not shown).

Effect of the "High-Ca^{2+} Ringer's on $\Delta[Ca^{2+}]$

The experiments described in the preceding section were carried out in a Ringer's solution containing 11.8 mM Ca^{2+} rather than the 1.8 mM Ca^{2+} level typically used in frog Ringer's. The higher Ca^{2+} level was used in most of our experiments because, on

average, fiber viability was increased somewhat if micro-injections of indicator were carried out in the high Ca^{2+} Ringer's. The use of a high Ca^{2+} Ringer's is not a requirement for a successful injection, however, as many previous experiments that used other indicator dyes were carried out in a 1.8 mM Ca^{2+} Ringer's. It was of interest to check the effect of the Ringer Ca^{2+} level on the recorded Ca^{2+} transients.

Fig. 8 shows a comparison of furaptra's $\Delta[Ca^{2+}]$ recorded from a fiber in normal Ca^{2+} Ringer's (1.8 mM; dotted trace) and in high Ca^{2+} Ringer's (11.8 mM; continuous trace). The two traces have very similar amplitudes, although the time course of $\Delta[Ca^{2+}]$ was delayed slightly in the high Ca^{2+} Ringer's. Similar results were seen in four other fibers. On average ($n = 5$), the peak amplitude of $\Delta[Ca^{2+}]$ in the high Ca^{2+} Ringer's was 1.035 (±0.034, SEM) times that observed in the normal Ca^{2+} Ringer's, a difference that is not significantly different from 1.0 ($P > 0.05$, two-tailed t test). In terms of time course, the $\Delta[Ca^{2+}]$ signals in the two Ringer solutions were significantly different ($P < 0.05$) with respect to two measures: (*a*) times to half-rise, 3.4 vs. 4.3 ms, with the average difference being 0.9 ± 0.2 ms; and (*b*) time-to-peak, 5.4 vs. 6.6 ms, with the average difference being 1.2 ± 0.4 ms (normal Ca^{2+} vs. high Ca^{2+}

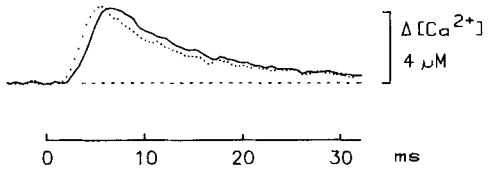

FIGURE 8. Effect of Ringer Ca^{2+} concentration on $\Delta[Ca^{2+}]$. The $\Delta F/F$ signal from furaptra was measured in the same fiber in an 11.8 mM $CaCl_2$ Ringer's, a 1.8 mM $CaCl_2$ Ringer's (*dotted trace*), and again in the high Ca^{2+} Ringer's. The two measurements of $\Delta[Ca^{2+}]$ in the high Ca^{2+} Ringer's had identical time courses but amplitudes that differed slightly (by 7%); the continuous trace is the average of these two measurements. Note that the action potential was initiated by a brief (0.5 ms) shock from a pair of extracellular electrodes positioned 1–2 mm from the site of optical recording. Fiber reference, 062889.2; sarcomere length, 3.6 μm; fiber diameter, 114 μm; 16.0°C; 36–42 min after dye injection; $[D_T] = 0.06$ mM.

Ringer's, respectively). There was no statistically significant difference in the half-widths of the waveforms (9.4 vs. 10.0 ms, respectively, with the average difference being 0.6 ± 0.5 ms).

It seems likely that some of the delay in the $\Delta[Ca^{2+}]$ waveform seen in the high Ca^{2+} Ringer's may be attributable to a delay in the arrival of the action potential within the field of optical recording, since an elevation in Ringer Ca^{2+} is expected to raise the threshold for the triggering of the action potential and possibly to decrease its propagation velocity. Some of the delay might also arise because of changes in the voltage-dependent process that links depolarization of the transverse-tubular membranes to Ca^{2+} release from the sarcoplasmic reticulum; for example, an elevation in Ringer $[Ca^{2+}]$ is known to shift the steady-state distribution of muscle charge movement to more depolarized levels (Schlevin, 1979).

Effect of Sarcomere Length on $\Delta[Ca^{2+}]$

A second way in which our experimental conditions departed from normal physiological conditions concerns the use of highly stretched fibers (sarcomere lengths of

3.6–4.1 μm vs. physiological sarcomere lengths of 2.2–2.6 μm). Earlier studies on frog single fibers injected with other Ca^{2+} indicator molecules (aequorin, Blinks et al., 1978; arsenazo III, Baylor et al., 1983*a*) have suggested that the amplitude of $\Delta[Ca^{2+}]$ is decreased slightly (10–40%) at sarcomere lengths approaching 4.0 μm compared with that observed at more physiological sarcomere lengths. Some uncertainty exists, however, about the exact magnitude of the effect because both aequorin and arsenazo III track $\Delta[Ca^{2+}]$ with a substantial kinetic delay (Neering and Wier, 1980; Baylor et al., 1983*b*); in addition, the stoichiometry of the reactions of both of these indicators with Ca^{2+} is complex (Blinks et al., 1978; Thomas, 1979; Palade and Vergara, 1982). We have therefore used the fluorescence signal from furaptra to re-examine the effect of sarcomere length on $\Delta[Ca^{2+}]$.

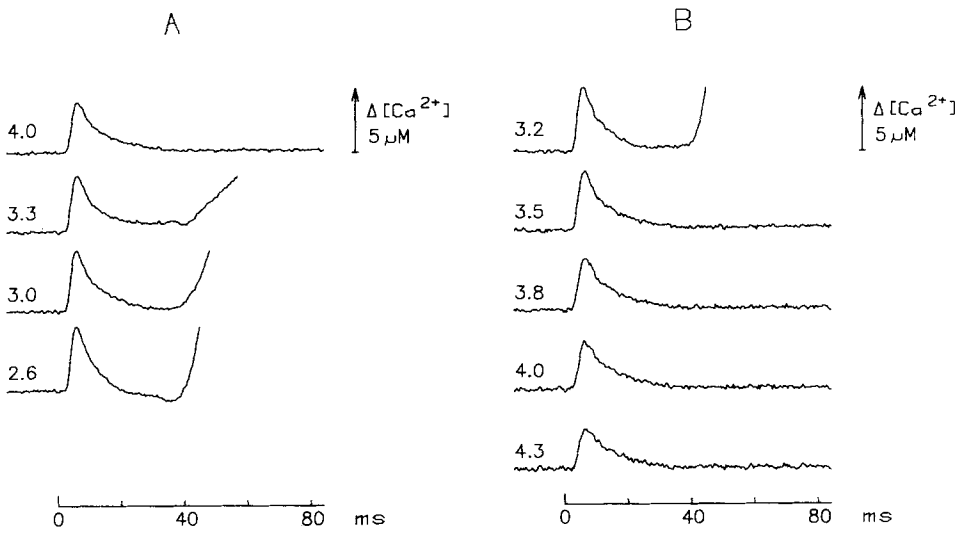

FIGURE 9. Furaptra's $\Delta[Ca^{2+}]$ signal recorded from a single fiber at different sarcomere lengths, indicated in micrometers next to each trace. The chronological order of the measurements was *A* before *B* and, within each part, from top to bottom. Traces at the shorter sarcomere lengths have been truncated after development of an obvious movement artifact. Fiber reference, 082989.2; fiber diameter, 78 μm (measured at sarcomere length = 3.8 μm); 16.2°C; 55–76 min after dye injection; $[D_T]$, 0.35–0.21 mM. Fluorescence measurements were collected from a 300-μm length of fiber at a fixed distance (1–2 mm) from the cathode of the stimulation electrodes.

Fig. 9 shows $\Delta[Ca^{2+}]$ signals recorded in the same fiber at a number of sarcomere lengths (indicated in micrometers to the left of each trace), and Fig. 10 summarizes results obtained from three fibers. In Fig. 10*A* the peak amplitude of $\Delta[Ca^{2+}]$ appears to increase somewhat as sarcomere length is shortened and to reach an approximately constant value at the shortest sarcomere lengths examined (2.5–2.8 μm). At 3.8 μm (the average sarcomere length routinely used in our experiments), the decrease in $\Delta[Ca^{2+}]$ is ~20% compared with the short sarcomere value, and at 4.3 μm, the longest sarcomere length examined, the decrease is ~30%. This effect of

sarcomere length on the peak amplitude of $\Delta[Ca^{2+}]$ is similar to that inferred previously from the other indicators (Blinks et al., 1978; Baylor et al., 1983*a*).

A new finding of our experiments with furaptra is that sarcomere length also produces a small but consistent change in the time to peak of $\Delta[Ca^{2+}]$ (Fig. 10 *B*) and probably also in the half-width of $\Delta[Ca^{2+}]$ (data not shown). In comparison with the values observed at 2.6–2.7 μm sarcomere length, the time to peak of $\Delta[Ca^{2+}]$ was increased by ~10% (0.5–0.6 ms) at 3.8 μm and by ~20% (1–1.2 ms) at 4.3 μm. Somewhat larger changes may apply to the half-width of $\Delta[Ca^{2+}]$, which was increased by ~20–30% at 3.8 μm and by ~35–45% at 4.3 μm. However, the precise magnitude of these latter changes was more difficult to ascertain because of possible contamination, at the shorter sarcomere lengths, of the falling phase of $\Delta[Ca^{2+}]$ by movement artifacts. These effects on the time course of $\Delta[Ca^{2+}]$ are not likely to be

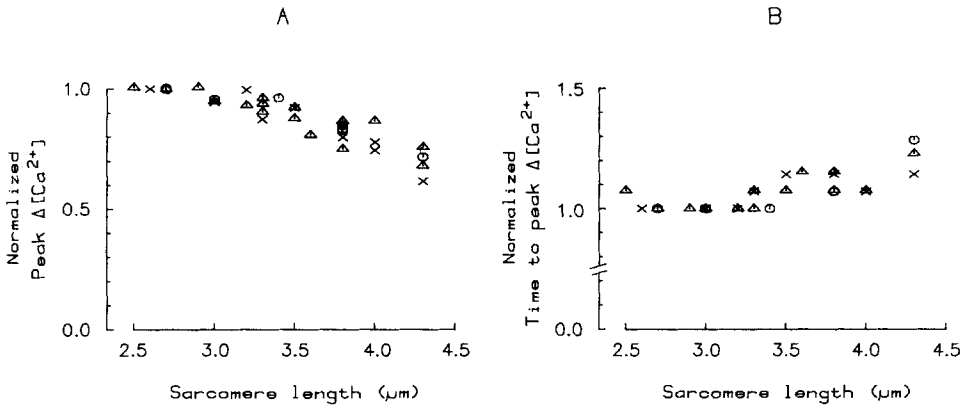

FIGURE 10. Summary of results from three fibers in which the normalized peak amplitude (*A*) and the normalized time-to-peak (*B*) of furaptra's $\Delta[Ca^{2+}]$ signal are plotted as a function of sarcomere length (cf. Fig. 9). In each part the data have been normalized by the value observed at sarcomere length 2.6–2.7 μm. Fiber references: 062889.1 (*triangles*), 062889.2 (*circles*), 082989.2 (*crosses*); 16.0–16.2°C; fiber diameters, 78–114 μm (measured at a sarcomere length near 3.8 μm); $[D_T] < 0.6$ mM. The normalization factors used were 4.1 μM and 5.2 ms (*triangles*), 5.5 μM and 5.6 ms (*circles*), and 5.0 μM and 5.6 ms (*crosses*) in *A* and *B*, respectively.

associated with differences in the conduction velocity of the action potential, which shows almost no variation with sarcomere length (Oetliker and Schumperli, 1982).

Likely Contribution of $\Delta[Mg^{2+}]$ to ΔF at Later Times after Stimulation

Previous work with azo-1 (Hollingworth and Baylor, 1986) and fura-2 (Baylor and Hollingworth, 1988), two high affinity Ca^{2+} indicators little influenced by physiological levels of Mg^{2+} and H^+, has indicated that at later times after a single action potential, $\Delta[Ca^{2+}]$ returns close to, but remains slightly elevated above, baseline. For example, 100–200 ms after stimulation, the quasi–steady-state elevation (denoted by $\Delta[Ca^{2+}]_{steady}$) averaged 0.01–0.02 of the peak change in $[Ca^{2+}]$ ($\Delta[Ca^{2+}]_{peak}$). Given Eqs. 3 and 4 in Methods and the assumption that furaptra's ΔF reflects $\Delta[Ca^{2+}]$ only, the value of $\Delta F_{steady}/\Delta F_{peak}$ (the quasi–steady-state ΔF divided by peak ΔF) is then

expected to be 0.011–0.022 if $\Delta F_{peak}/\Delta F_{max}$ is 0.094 (the average value observed for this parameter for the fibers in Table II; not shown). The range 0.011–0.022 is significantly smaller ($P < 0.01$, two-tailed t test) than the average value actually measured for $\Delta F_{steady}/\Delta F_{peak}$, 0.053 ± 0.004 (column 9 of Table II). The difference between 0.053 and 0.011–0.022 presumably reflects some myoplasmic event(s) other than $\Delta[Ca^{2+}]$, to which furaptra is sensitive.

A likely explanation for the extra component of $\Delta F_{steady}/\Delta F_{peak}$ is an increase in myoplasmic free $[Mg^{2+}]$, $\Delta[Mg^{2+}]$. Previous work, both computational and experimental, has indicated that an increase in $[Mg^{2+}]$ probably begins during the falling phase of $\Delta[Ca^{2+}]$ and reaches a quasi–steady-state elevation by ~100 ms after a single action potential (Gillis et al., 1982; Baylor et al., 1983*a*, 1985*b*; Cannell and Allen, 1984; Maylie et al., 1987*b*; Baylor and Hollingworth, 1988; Irving et al., 1989). At 16–18°C the experimental estimates for the $\Delta[Mg^{2+}]$ observed 100–200 ms after stimulation (denoted by $\Delta[Mg^{2+}]_{steady}$) are in the range 45–70 μM (Baylor et al., 1985*b*; Irving et al., 1989). These latter estimates are close to that calculated for $\Delta[Mg^{2+}]$ if: (*a*) the principal source of $\Delta[Mg^{2+}]$ is the Mg^{2+} released from parvalbumin in exchange for Ca^{2+} bound during the Ca^{2+} transient, and (*b*) approximately two-thirds of the released Mg^{2+} is bound by other Mg^{2+}-buffer sites (e.g., those on phosphocreatine), with the other one-third remaining free. For example, if it is assumed that (*a*) $\Delta[Ca^{2+}]$ peak is 10 μM (cf. Discussion), (*b*) the waveform of $\Delta[Ca^{2+}]$ is similar to that given in Fig. 6 *B*, and (*c*) $\Delta[Ca^{2+}]_{steady}/\Delta[Ca^{2+}]_{peak}$ is 0.015, the predicted $\Delta[Mg^{2+}]_{steady}$, calculated as described in Baylor and Hollingworth (1988), is 80–90 μM.

On the other hand, the unexplained component of furaptra's $\Delta F_{steady}/\Delta F_{peak}$, 0.031–0.042, corresponds to a $\Delta[Mg^{2+}]_{steady}$ of 20–30 μM if calibrated by the constants given in Methods and the assumption that f_{MgD} for furaptra is 0.1. Since the 20–30 μM estimate for $\Delta[Mg^{2+}]_{steady}$ is smaller than the range of values, 45–90 μM, estimated from the experimental and computational work described above, these various observations may be reconciled under the supposition that either the earlier estimates of $\Delta[Mg^{2+}]_{steady}$ are too large or the effective value of $K_{d,Mg}$ for furaptra in myoplasm is larger than the 5.3 mM value measured in the in vitro calibrations.

ΔF in Response to Repetitive Stimulation

In several experiments, furaptra's ΔF signal was measured in response to a brief, high-frequency train of action potentials. Results from one such experiment are shown in Fig. 11. The superimposed traces in *A* show ΔF recordings on a fast time base in response to 1, 5, 10, and 20 shocks given at 104 Hz (9.6 ms between successive shocks). It is apparent that the first shock produced the largest single peak in ΔF and that successive peaks decayed to a steady level somewhat smaller than the first peak; on average, 77% of the first peak, for peaks 5–20. Although this was the only experiment in which a 20-shock train was given, 5- and 10-shock trains were recorded in five other similar experiments, for which the range of values of $[D_T]$ was 0.13–0.80 mM. On average ($n = 6$), the amplitudes of the fifth and tenth ΔF peaks compared with that of the first peak were 98 ± 9 and 90 ± 10%, respectively (stimulation frequencies, 100–104 Hz). Since, as indicated in the previous section, there is likely to be a significant contribution to ΔF at later times after stimulation due to a rise in $[Mg^{2+}]$, the results imply that the peak of $\Delta[Ca^{2+}]$, on average, shows little

or no summation during a brief high-frequency tetanus; rather, the peaks typically decay somewhat in comparison with the first peak. This conclusion is very similar to that reached previously from intact fibers micro-injected with antipyrylazo III (Quinta-Ferreira et al., 1984; Baylor and Hollingworth, 1988) and from cut fibers exposed to either antipyrylazo III (Maylie et al., 1987*b*) or to three dyes from the purpurate family of Ca^{2+} indicators (Maylie et al., 1987*a*; Hirota et al., 1989).

It is also apparent in Fig. 11 *A* that after cessation of stimulation the later, quasi–steady-state elevation of ΔF increased with the number of stimulated action potentials. For the six experiments, $\Delta F_{steady}/\Delta F_{peak}$ (the mean value of ΔF during the period 100–200 ms after the last shock compared with the peak of ΔF due to the first shock) averaged 0.054 ± 0.008 for a single shock, 0.113 ± 0.023 for the 5-shock

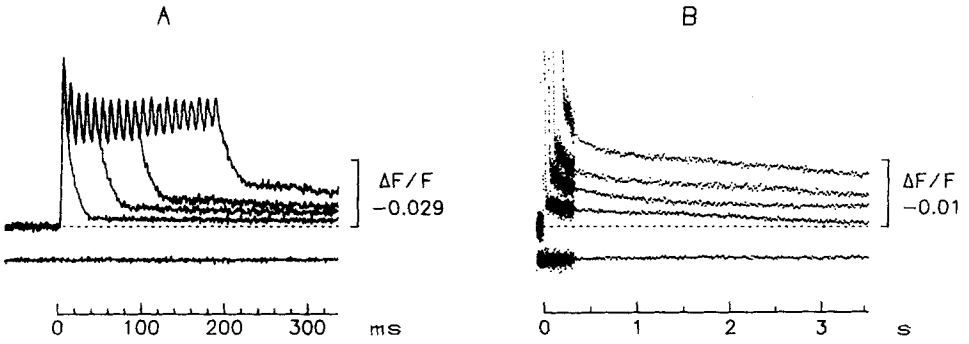

FIGURE 11. Furaptra fluorescence signals from a fiber stimulated by 1, 5, 10, and 20 action potentials separated by 9.6 ms. The traces are displayed at low gain on a fast time base (*A*) and at higher gain on a slow time base (*B*). The lowermost record in each part was obtained in the absence of stimulation and is a control for lamp stability. In *A*, data sampling was every 0.8 ms. In *B*, data sampling was every 0.8 ms for the first 0.4 s and every 12.8 ms for the remainder of the trace. (The lower noise level apparent for the latter sampling interval reflects the fact that each of these data points is an average of 16 points taken every 0.8 ms.) The 1-shock trace is an average of three identical sweeps; the 5-shock, two sweeps; the 10- and 20-shocks, a single sweep each; and the unstimulated response, four sweeps. Fiber no., 082989.2; fiber diameter, 76 μm; sarcomere length, 4.0 μm; 16.1°C; 37–44 min after injection; $[D_T]$ = 0.40 mM.

train, and 0.149 ± 0.031 for the 10-shock train. For the single experiment with a 20-shock train, $\Delta F_{steady}/\Delta F_{peak}$ was 0.229.

As discussed in the preceding section, the value of $\Delta F_{steady}/\Delta F_{peak}$ probably reflects contributions from elevated myoplasmic levels of both $[Ca^{2+}]$ and $[Mg^{2+}]$. Since, as judged from experiments with fura-2 alone (Baylor, S. M., and S. Hollingworth, unpublished observations), the amplitude of $\Delta[Ca^{2+}]_{steady}$ is also increased about two- and threefold, respectively, for 5- and 10-shock trains, the results from the furaptra experiments are consistent with the hypothesis that the relative contributions of $\Delta[Ca^{2+}]$ and $\Delta[Mg^{2+}]$ to the ΔF_{steady} signal remain approximately constant as the number of stimulations is varied.

Fig. 11 *B* shows the furaptra ΔF signals from *A* on a higher vertical gain and a

10-fold slower sweep speed. Even several seconds after stimulation, the return of ΔF to baseline is incomplete, and, at least for the case of multiple stimulation, the data suggest that it probably takes longer than 10 s for the resting state of the fiber to be restored. In four other fibers subjected to 5- and 10-shock trains and studied on a second time scale, ΔF showed an incomplete return to baseline, with a time course very similar to that shown in Fig. 11 *B*.

DISCUSSION

Comparison of Furaptra with Other Ca^{2+} Indicator Dyes

The experiments of this paper show that, in comparison with other indicators previously used in skeletal muscle fibers, furaptra is quite useful for tracking $\Delta[Ca^{2+}]$ in response to electrical stimulation. First, the percentage of indicator that appears to be bound to myoplasmic constituents of large molecular weight is smaller for furaptra (42–51%) than for either fura-2 (60–85%, Baylor and Hollingworth, 1988; Konishi et al., 1988), antipyrylazo III (~75%, Baylor et al., 1986, Maylie et al., 1987*b*), or azo-1 (~90%, Baylor et al., 1986), although not as small as that estimated for PDAA (24–43% in intact fibers, Konishi and Baylor, 1991; 19% in cut fibers, Hirota et al., 1989). Thus, the calibration of furaptra's $\Delta[Ca^{2+}]$ is probably more accurate than that of fura-2, antipyrylazo III, and azo-1, although probably not as accurate as that of PDAA.

Second, the effective K_d of furaptra for Ca^{2+} under intracellular conditions appears to represent a good compromise in terms of the unavoidable trade-off between signal size and response linearity (for a fixed concentration of indicator). For example, Δf_{CaD} (the fraction of the indicator that is driven into the Ca^{2+}-bound form during activity) is typically 0.1 for furaptra, which is much smaller than the 0.7 value seen with fura-2 but 5–20-fold larger than the values typically seen with PDAA or antipyrylazo III, 0.005–0.02.

Third, furaptra's absorbance or fluorescence change (ΔA or ΔF) appears to track $\Delta[Ca^{2+}]$ with little or no kinetic delay (cf. Figs. 5 and 6). In this regard, furaptra represents a great improvement over fura-2 and a slight improvement over antipyrylazo III (cf. Baylor and Hollingworth, 1988). A rapid kinetic response is in fact expected given the K_d of furaptra for Ca^{2+} measured in the in vitro calibrations (cf. Figs. 1 and 2). At 44 μM furaptra's K_d is ~250-fold greater than that of fura-2. If the on-rate constants are similar for the Ca^{2+} complexation reactions of these indicators, then the lower affinity of furaptra implies a 250-fold larger off-rate constant. Under in vivo conditions, fura-2's off-rate constant has been estimated to be ~20 s^{-1} at 16°C (Baylor and Hollingworth, 1988); thus furaptra's off-rate constant in vivo may be ~5,000 s^{-1}. This rate, in turn, implies that $\Delta[Ca^{2+}]$ estimated with furaptra should track the true $\Delta[Ca^{2+}]$ waveform with a delay of no more than 0.2 ms (=1/5,000 s^{-1}). On the other hand, the experiments that directly compared $\Delta[Ca^{2+}]$ from furaptra with that from PDAA (e.g., Fig. 6) raised the possibility of a slightly greater delay, 1–2 ms. If real, the extra delay may be related to the likelihood that the true myoplasmic $\Delta[Ca^{2+}]$ has significant spatial nonuniformity (Cannell and Allen, 1984). As discussed by Hirota et al. (1989), a very low affinity indicator like PDAA (K_d = 0.9 mM) is expected to accurately monitor the spatially averaged $\Delta[Ca^{2+}]$, whereas a higher-

affinity indicator like furaptra may track this $\Delta[Ca^{2+}]$ with some nonlinearity in addition to that implied by Eq. 4. Another consideration is that the effective rates of furaptra's reaction with Mg^{2+} may not be instantaneous on the time scale of $\Delta[Ca^{2+}]$ and thus may contribute to the observed kinetics of the furaptra signal. This possibility arises because, for identical K_d's, Mg^{2+} reaction rates are generally two to three orders of magnitude slower than Ca^{2+} rates (Diebler et al., 1969) and a small, but not entirely negligible, fraction of furaptra is likely to be in the Mg^{2+}-bound form in resting fibers (cf. Methods). By itself, however, a delay in the re-equilibration of indicator between Mg^{2+}-bound and metal-free states in response to $\Delta[Ca^{2+}]$ will not explain the 1–2-ms delay (if real), since this re-equilibration reaction should produce a signal of opposite polarity to the initial signal and should therefore speed up rather than retard the early falling phase of the furaptra signal.

Fourth, since a change in fluorescence is generally less susceptible to interference from movement artifacts and fiber intrinsic changes than is a change in absorbance (cf. Fig. 5), furaptra's ΔF represents a significant improvement over the ΔA's available from both PDAA and antipyrylazo III, which require that measurements be made at several wavelengths to estimate the dye-related signal with confidence (cf. Fig. 6).

A final comparison concerns possible interfering effects from changes in myoplasmic free $[Mg^{2+}]$. Because of the very large selectivity of fura-2 for Ca^{2+} over Mg^{2+} (in vitro K_d's of 0.14 μM and 10 mM, respectively; Grynkiewicz et al., 1985), the contribution of $\Delta[Mg^{2+}]$ to the late ΔF from fura-2 is very probably negligible. Furaptra, however, prefers Ca^{2+} over Mg^{2+} by only a factor of ~120 (at 16°C). Since, in response to a single action potential, $\Delta[Mg^{2+}]$ probably increases during the falling phase of $\Delta[Ca^{2+}]$ (Baylor et al., 1985*b*; Irving et al., 1989), it is expected that the later phase of furaptra's ΔF will have a contribution from $\Delta[Mg^{2+}]$ as well as $\Delta[Ca^{2+}]$. In fact, evidence for a non-Ca^{2+} contribution to furaptra's ΔF at later times was obtained in the experiments (cf. Fig. 11 and associated discussion). The amplitude of the extra ΔF, if calibrated in $\Delta[Mg^{2+}]$ units, corresponded to 20–30 μM. This range is about twofold smaller than previous experimental estimates of $\Delta[Mg^{2+}]$ obtained with antipyrylazo III at wavelengths with little sensitivity to Ca^{2+} (Baylor et al., 1985*b*; Irving et al., 1989). In terms of the Mg^{2+} interference in the late Ca^{2+}-related absorbance change measured with the indicators PDAA and antipyrylazo III, a precise evaluation is made difficult for two reasons: (*a*) the expected contribution from a $\Delta[Mg^{2+}]$ of 20–60 μM, while undoubtedly small, is not readily calculable for either antipyrylazo III or PDAA from the published in vitro calibrations (cf. Hirota et al., 1989 for PDAA, and Rios and Schneider, 1981 and Baylor et al., 1986 for antipyrylazo III); and (*b*) in vivo, there is already significant experimental uncertainty at late times in the absorbance signals owing to the corrections for fiber intrinsic changes.

Probable Pharmacological Alteration of the Time Course of $\Delta[Ca^{2+}]$ by Larger Concentrations of Antipyrylazo III

In fibers injected with PDAA at concentrations up to 5 mM (Konishi and Baylor, 1991) or with furaptra at concentrations up to 0.5 mM (cf. Table II and Fig. 7 *B*), the average value for the half-width of $\Delta[Ca^{2+}]$ was 8–10 ms. An essentially identical value was found in fibers containing relatively small concentrations of antipyrylazo III

(<0.6 mM) (Baylor and Hollingworth, 1988; this article). However, at millimolar concentrations of antipyrylazo III, a striking increase in the average half-width of $\Delta[Ca^{2+}]$ is seen; e.g., to ~20 ms at 1–2 mM indicator (Baylor et al., 1983*b*; Baylor and Hollingworth, 1988). (Note that for these comparisons, all indicator concentrations have been referred to the myoplasmic water volume; cf. Baylor et al., 1983*a*.) This increase in half-width cannot be attributed to a simple Ca^{2+}-buffering effect of antipyrylazo III, since an equivalent amount of buffering by furaptra and PDAA produced only a 1–2-ms increase in the half-width of $\Delta[Ca^{2+}]$. Thus, low millimolar concentrations of antipyrylazo III appear to have a pharmacological effect on the time course of $\Delta[Ca^{2+}]$ that is not shared by PDAA or furaptra. The most likely possibilities to explain this action are that (*a*) the time course of Ca^{2+} release from the sarcoplasmic reticulum is prolonged; e.g., antipyrylazo III may delay the rate at which the sarcoplasmic reticulum Ca^{2+} channels close in response to repolarization of the surface and transverse-tubular membranes, or (*b*) the rate of Ca^{2+} removal from the myoplasm is reduced; e.g., antipyrylazo III may have an inhibitory effect on the sarcoplasmic reticulum Ca^{2+}-ATPase.

Summary of Properties of $\Delta[Ca^{2+}]$ in Response to Action Potential Stimulation

This section summarizes properties about $\Delta[Ca^{2+}]$ inferred from intact fibers at 16°C injected with minimally perturbing concentrations of furaptra, PDAA, antipyrylazo III, azo-1, or fura-2.

(*a*) As confirmed by furaptra, PDAA, and antipyrylazo III, the average time course of $\Delta[Ca^{2+}]$ in response to a single action potential is characterized by a time to half-rise of 4–4.5 ms, a time to peak of 6–7 ms, and a half-width of 8–10 ms. (Note that the time to half-rise and time to peak, but not the half-width, of $\Delta[Ca^{2+}]$ would be ~1 ms less if measured in a 1.8 mM rather than 11.8 mM $[Ca^{2+}]$ Ringer's solution.)

(*b*) The indicators do not agree on the average peak amplitude of $\Delta[Ca^{2+}]$. The values calibrated from PDAA, furaptra, antipyrylazo III, fura-2, and azo-1 are ~10, 5, 2, 1–2, and 1–2 μM, respectively. (Note that the latter three values reflect corrections of the ΔA or ΔF measurements for kinetic delays inherent in the in vivo Ca^{2+}-dye reaction.) The value calibrated from PDAA is probably the most reliable since the percentage of PDAA that is bound to myoplasmic constituents (24–44%) appears to be somewhat smaller than that of furaptra (42–51%) and considerably smaller than that of antipyrylazo III (~75%), fura-2 (~75%), and azo-1 (~90%). With furaptra, the calibration of $\Delta[Ca^{2+}]$ is likely to be erroneously small if bound furaptra has its K_d for Ca^{2+} altered in a similar fashion as bound fura-2 (to which it is structurally similar). As shown in Konishi et al. (1988), metal-free fura-2, when bound to aldolase, an abundant cytoplasmic protein, has a slightly red-shifted absorbance spectrum and an enhanced fluorescence intensity, and reacts with Ca^{2+} with a nearly fourfold larger K_d. Moreover, in vivo the fura-2 Ca^{2+} signal probably arises from both protein-bound and protein-free indicator molecules, which appear to be in a rapid kinetic equilibrium on the time scale of $\Delta[Ca^{2+}]$. Since in vivo approximately half of furaptra appears to be bound to relatively immobile myoplasmic constituents, it follows that the calibration of its $\Delta F/F$ in terms of $\Delta[Ca^{2+}]$ may be too small by about a factor of two (cf. Fig. 8 *A* of Konishi et al., 1988). Thus, both a corrected furaptra calibration

and a straightforward PDAA calibration place the average peak value of $\Delta[Ca^{2+}]$ at ~10 μM. A reasonable working hypothesis is that the true peak value lies in the range 5–20 μM.

(*c*) At later times in the transient, ~100–200 ms after stimulation, $\Delta[Ca^{2+}]$ has returned close to, but remains slightly elevated above, baseline. The most reliable estimates of this quasi–steady-state elevation have been obtained with azo-1 and fura-2. Although neither azo-1 nor fura-2 tracks $\Delta[Ca^{2+}]$ with rapid kinetics, both indicators are quite insensitive to influences from $\Delta[Mg^{2+}]$ and ΔpH, and fura-2 is quite insensitive to movement artifacts and fiber intrinsic changes. With both indicators, the amplitude of the maintained phase of $\Delta[Ca^{2+}]$ was ~0.01–0.02 of the peak amplitude of $\Delta[Ca^{2+}]$ (estimated after appropriate kinetic corrections; Hollingworth and Baylor, 1986; Baylor and Hollingworth, 1988). Thus, if peak $\Delta[Ca^{2+}]$ averages 10 μM, maintained $\Delta[Ca^{2+}]$ 100–200 ms after stimulation averages 0.1–0.2 μM.

(*d*) The peak value of $\Delta[Ca^{2+}]$ measured at shorter sarcomere lengths, e.g., 2.5–2.8 μm, is likely to be ~25% larger than the value measured at 3.8 μm, the average sarcomere length of our studies (cf. Fig. 10 *A*). Moreover, the time to peak and probably the half-width of $\Delta[Ca^{2+}]$ would be slightly less if measured at physiological sarcomere length (cf. Fig. 10 *B*).

(*e*) When fibers are stimulated by a high-frequency train of action potentials, the most common finding is that the peak of $\Delta[Ca^{2+}]$ is maximal as a result of the first shock, and that peaks resulting from subsequent shocks decline somewhat in amplitude relative to the first peak (cf. Fig. 11 *A*). At late times after stimulation, 0.1 to several seconds, $\Delta[Ca^{2+}]$ and $\Delta[Mg^{2+}]$ increase monotonically with the number of shocks in the train. The return of these changes to baseline probably takes longer than 10 s (cf. Fig. 11 *B* and associated discussion).

We thank Dr. W. K. Chandler and Dr. P. C. Pape for comments on the manuscript.

Financial support was provided by the U. S. National Institutes of Health (grant NS-17620 to S. M. Baylor).

Original version received 12 April 1990 and accepted version received 30 July 1990.

REFERENCES

Alvarez-Leefmans, E. J., S. M. Gamino, F. Giraldez, and H. Gonzalez-Serratos. 1986. Intracellular free magnesium in frog skeletal muscle fibres measured with ion-selective micro-electrodes. *Journal of Physiology.* 378:461–483.

Baylor, S. M., W. K. Chandler, and M. W. Marshall. 1981. Studies in skeletal muscle using optical probes of membrane potential. *In* Regulation of Muscle Contraction: Excitation-Contraction Coupling. A. D. Grinnell and Mary A. B. Brazier, editors. Academic Press, New York. 97–130.

Baylor, S. M., W. K. Chandler, and M. W. Marshall. 1982*a*. Optical measurements of intracellular pH and magnesium signals in frog skeletal muscle fibres. *Journal of Physiology.* 331:105–137.

Baylor, S. M., W. K. Chandler, and M. W. Marshall. 1982*b*. Use of metallochromic dyes to measure changes in myoplasmic calcium during activity in frog skeletal muscle fibers. *Journal of Physiology.* 331:139–177.

Baylor, S. M., W. K. Chandler, and M. W. Marshall. 1983*a*. Sarcoplasmic reticulum calcium release in frog skeletal muscle fibres estimated from Arsenazo III calcium transients. *Journal of Physiology*. 344:625–666.

Baylor, S. M., and S. Hollingworth. 1988. Fura-2 calcium transients in frog skeletal muscle fibres. *Journal of Physiology*. 403:151–192.

Baylor, S. M., and S. Hollingworth. 1990. Absorbance signals from resting frog skeletal muscle fibers injected with the pH indicator dye phenol red. *Journal of General Physiology*. 96:449–471.

Baylor, S. M., S. Hollingworth, C. S. Hui, and M. E. Quinta-Ferreira. 1985*a*. Calcium transients from intact frog skeletal muscle fibres simultaneously injected with Antipyrylazo III and Azol. *Journal of Physiology*. 365:70P.

Baylor, S. M., S. Hollingworth, C. S. Hui, and M. E. Quinta-Ferreira. 1986. Properties of the metallochromic dyes Arsenazo III, Antipyrylazo III and Azo-1 in frog skeletal muscle fibres at rest. *Journal of Physiology*. 377:89–141.

Baylor, S. M., S. Hollingworth, and M. Konishi. 1989. Calcium transients in intact frog single skeletal muscle fibres measured with the fluorescent indicator dye Mag-fura-2. *Journal of Physiology*. 418:69P.

Baylor, S. M., M. E. Quinta-Ferreira, and C. S. Hui. 1983*b*. Comparison of isotropic calcium signals from intact frog muscle fibers injected with Arsenazo III or Antipyrylazo III. *Biophysical Journal*. 44:107–112.

Baylor, S. M., M. E. Quinta-Ferreira, and C. S. Hui. 1985*b*. Isotropic components of Antipyrylazo III signals from frog skeletal muscle fibers. *In* Calcium in Biological Systems. R. P. Rubin, G. Weiss, and J. W. Putney, Jr., editors. Plenum Publishing Corp., New York. 339–349.

Blatter, L. A. 1990. The role of a Na/Mg exchange mechanism in the regulation of intracellular free magnesium in frog skeletal muscle. *Biophysical Journal*. 57:533*a*. (Abstr.)

Blinks, J. R., R. Rudel, and S. R. Taylor. 1978. Calcium transients in isolated amphibian skeletal muscle fibres: detection with aequorin. *Journal of Physiology*. 227:291–323.

Cannell, M. B., and D. G. Allen. 1984. Model of calcium movements during activation in the sarcomere of frog skeletal muscle. *Biophysical Journal*. 45:913–925.

Cantor, C. R., and P. R. Schimmel. 1980. Biophysical Chemistry. Part II. W. H. Freeman and Company, San Francisco. 347 pp.

Crank, J. 1956. The Mathematics of Diffusion. Oxford University Press, London.

Diebler, H., M. Eigen, G. Ilgenfritz, G. Maas, and R. Winkler. 1969. Kinetics and mechanism of reactions of main group metal ions with biological carriers. *Pure and Applied Chemistry*. 20:93–115.

Gillis, J. M., D. Thomason, J. Lefevre, and R. H. Kretsinger. 1982. Parvalbumins and muscle relaxation: a computer simulation study. *Journal of Muscle Research and Cell Motility*. 3:377–398.

Grynkiewicz, G., M. Poenie, and R. Y. Tsien. 1985. A new generation of Ca^{2+} indicators with greatly improved fluorescence properties. *Journal of Biological Chemistry*. 260:3440–3450.

Hirota, A., W. K. Chandler, P. L. Southwick, and A. S. Waggoner. 1989. Calcium signals recorded from two new purpurate indicators inside frog cut twitch fibers. *Journal of General Physiology*. 94:597–631.

Hollingworth, S., R. W. Aldrich, and S. M. Baylor. 1987. In vitro calibration of the equilibrium reactions of the metallochromic indicator dye antipyrylazo III with calcium. *Biophysical Journal*. 51:383–393.

Hollingworth, S., and S. M. Baylor. 1986. Calcium transients in frog skeletal muscle fibers injected with Azo-1. *In* Optical Methods in Cell Physiology. P. DeWeer and B. M. Salzberg, editors. John Wiley & Sons, Inc., New York. 261–263.

Hollingworth, S., and S. M. Baylor. 1990. Changes in phenol red absorbance in response to electrical stimulation of frog skeletal muscle fibers. *Journal of General Physiology*. 96:473–491.

Irving, M., J. Maylie, N. L. Sizto, and W. K. Chandler. 1989. Simultaneous monitoring of changes in magnesium and calcium concentrations in frog cut twitch fibers containing Antipyrylazo III. *Journal of General Physiology.* 93:585–608.

Konishi, M., and S. M. Baylor. 1991. Myoplasmic calcium transients monitored with purpurate indicator dyes injected into intact frog skeletal muscle fibers. *Journal of General Physiology.* 97:245–270.

Konishi, M., S. Hollingworth, and S. M. Baylor. 1989. Calcium transients in frog skeletal muscle fibers measured with the fluorescent "magnesium" indicator, Mag-fura-2. *Journal of General Physiology.* 94:13*a*. (Abstr.)

Konishi, M., S. Hollingworth, and S. M. Baylor. 1990. Myoplasmic calcium transients in intact frog twitch fibers monitored with furaptra (= Mag-fura-2) and purpurate-diacetic acid (= PDAA). *Biophysical Journal.* 57:344*a*. (Abstr.)

Konishi, M., A. Olson, S. Hollingworth, and S. M. Baylor. 1988. Myoplasmic binding of Fura-2 investigated by steady-state fluorescence and absorbance measurements. *Biophysical Journal.* 54: 1089–1104.

Kushmerick, M. J., and R. J. Podolsky. 1969. Ionic mobility in muscle cells. *Science.* 166:1297–1298.

Martell, A. E., and R. M. Smith. 1974. Critical Stability Constants. Vol. 1: Amino Acids. Plenum Publishing Corp., New York. 199–269.

Maylie, J., M. Irving, N. L. Sizto, G. Boyarsky, and W. K. Chandler. 1987*a*. Optical signals obtained with tetramethylmurexide in cut frog twitch fibers. *Journal of General Physiology.* 89:145–176.

Maylie, J., M. Irving, N. L. Sizto, and W. K. Chandler. 1987*b*. Optical signals obtained with Antipyrylazo III in cut frog twitch fibers. *Journal of General Physiology.* 89:83–143.

Neering, J. R., and W. G. Wier. 1980. Kinetics of aequorin luminescence after step changes in $[Ca^{2+}]$: significance for interpretation of intracellular aequorin signals. *Federation Proceedings.* 39:1806.

Oetliker, H., and R. A. Schumperli. 1982. Influence of sarcomere length, tonicity and external sodium concentration of conduction velocity in frog muscle fibres. *Journal of Physiology.* 332:203–221.

Palade, P., and J. Vergara. 1982. Arsenazo III and antipyrylazo III calcium transients in single skeletal muscle fibers. *Journal of General Physiology.* 79:679–707.

Quinta-Ferreira, M. E., S. M. Baylor, and C. S. Hui. 1984. Antipyrylazo III (Ap III) and arsenazo III (Az III) calcium transients from frog skeletal muscle fibers simultaneously-injected with both dyes. *Biophysical Journal.* 45:47*a*. (Abstr.)

Raju, B., E. Murphy, L. A. Levy, R. D. Hall, and R. E. London. 1989. A fluorescent indicator for measuring cytosolic free magnesium. *American Journal of Physiology.* 256:C540–C548.

Rios, E., and M. F. Schneider. 1981. Stoichiometry of the reactions of calcium with the metallochromic indicators antipyrylazo III and arsenazo III. *Biophysical Journal.* 36:607–621.

Schlevin, H. H. 1979. Effects of external calcium concentration and pH on charge movement in frog skeletal muscle. *Journal of Physiology.* 288:129–158.

Thomas, M. V. 1979. Arsenazo III forms 2:1 complexes with Ca and 1:1 complexes with Mg under physiological conditions. *Biophysical Journal.* 25:541–548.